



ADDIS ABABA UNIVERSITY
ADDIS ABABA INSTITUTE OF TECHNOLOGY
SCHOOL OF GRADUATE STUDIES

**SIMULATION OF OEDOMETER TEST USING FINITE
ELEMENT METHOD**

**A Thesis Submitted to the School Of Graduate Studies of Addis Ababa University in
Partial Fulfillment of the Requirements for the Degree of Masters of Science in Civil
Engineering (Geotechnical Engineering)**

By: YONAS TESFAY

**Addis Ababa University
Addis Ababa, Ethiopia
November, 2018**

SIMULATION OF OEDOMETER TEST USING FINITE ELEMENT METHOD

By: YONAS TESFAY

A Thesis Submitted to the School Of Graduate Studies of Addis Ababa University
in Partial Fulfillment of the Requirements for the Degree of

Masters of Science

in

Civil Engineering

Geotechnical Engineering

Advisor

Dr.-Ing Henok Fikre

Simulation of Oedometer test using Finite Element Method

ADDIS ABABA UNIVERSITY
ADDIS ABABA INSTITUTE OF TECHNOLOGY
SCHOOL OF CIVIL AND ENVIRONMENTAL ENGINEERING

This is to certify that the thesis prepared by Yonas Tesfay, entitled: Simulation of Oedometer test using finite element method and submitted in partial fulfillment of the requirements for the degree of Master of Sciences (Civil Engineering) complies with the regulations of the University and meets the accepted standards with respect to originality and quality.

Signed by the Examining Committee:

_____	_____	_____
Advisor	Signature	Date
_____	_____	_____
Internal Examiner	Signature	Date
_____	_____	_____
External Examiner	Signature	Date
_____	_____	_____
Chairman	Signature	Date

Declaration

I, the undersigned, declare that this thesis is my original work performed under the supervision of my research advisor Dr. –Ing. Henok Fikre and has not been presented for a degree in any other university. All sources of materials used for this thesis have been duly acknowledged.

Name: Yonas Tesfay

Signature: _____

Place: Addis Ababa Institute of Technology

Date of Submission:

Acknowledgement

I would like to express my sincere and deepest thank to my advisor Dr. –Ing. Henok Fikre for his unlimited support, close guidance and consultation he provides since the very beginning of title selection to final date of submission. His welcoming approach and advice has made the way of communication very easy and attractive.

My special thank goes to Admassu Tirualem for his endless support during the time of laboratory test early from the beginning to the end. I would also like to express my gratitude to Anteneh Mitku for his unforgettable support during the time of laboratory tests.

I am very grateful to my friends, Fsaha Kiros, Hagos Mekonen and Tesfay G/meskel for motivating me to start my thesis work and for their closer intimacy that they showed for the past two years.

Dedicated to my mother

Lemlem Ayele

Abstract

One-dimensional consolidation test is one of the commonly conducted laboratory tests used to determine the stiffness and compression properties of fine grained soils. Study on predicting bearing capacity and compressibility of clay soils is still attracting interests of geotechnical researchers. Besides the laboratory or field tests, finite element method is used increasingly to deal with such problems.

Abaqus 2D finite element software is used in this Thesis to simulate the one-dimensional consolidation (Oedometer) test which were conducted on cohesive specimens of red clay soils collected from Adisu Gebeya, Kolfe and Rufael area. In the finite element analysis, a constitutive soil model, Modified Drucker-Prager / Cap plasticity were used to simulate the Oedometer test. An axisymmetric finite element model using the program Abaqus is used in order to establish numerical models and analysis procedures that help to simulate the actual Oedometer test.

Appropriate boundary conditions were taken in to account during setting of the finite element models to simulate the actual no lateral displacement of the test in the laboratory. The applied pressures on the one-dimensional cell were also presented as a uniform distributed load and are loaded incrementally based on their magnitude on the top of the models.

The measured settlements at the end of Oedometer tests were observed close to the calculated values from the finite element analysis. Compressibility curves for the red clay specimens were generated considering three different cases from the finite element analysis and compared with the curves obtained from the laboratory. From these curves a corresponding strain for the additional pressure exerted due to the proposed structure can be determined easily. Hence, the results obtained from the finite element analysis can be used for preliminary design of foundations.

KEY WORDS: *Constitutive model, Finite Element Method (FEM), Cap hardening, Oedometer test.*

Table of content

Declaration..... i

Acknowledgement.....VI

Abstract.....VIII

Table of content..... IX

List of symbols..... XII

List of figures.....XV

List of tables.....XVII

Chapter 1: Introduction 1

1.1 Background..... 1

1.2 Statement of the problem 3

1.3 Objective 3

1.3.1 General Objective 3

1.3.2 Specific Objectives 3

1.4 Methodology 3

1.5 Scope of the study..... 4

1.6 Organization of the thesis..... 4

Chapter 2: Literature review 5

2.1 Fundamental studies of clay soil behaviors 5

2.2 Origin and mineralogical composition of redclay soils..... 5

2.3 Red clay soil distribution in Addis Ababa 6

2.4 Atterberg limits 6

2.5 Consolidation of soils 8

2.5.1 Principle of consolidation 8

2.5.2 Consolidation theory.....	8
2.5.3 One-Dimensional consolidation test	13
2.5.2 Incremental Loading (IL) test.....	14
2.5.3 Constant rate of strain test (CRS)	15
2.5.4 Pre-Consolidation pressure (Pc)	15
2.5.5 Compression and Re-compression indecis.....	16
2.5.6 Consolidation properties of Addis Ababa red clay	16
2.6 Constitutive models.....	20
2.6.1 General.....	20
2.7 Related studies.....	20
Chapter 3: One- Dimensional Consolidation (Oedometer) tests and results	23
3.1 General.....	23
3.2 One - Dimensional Consolidation (Oedometer) test	23
3.3 Pre-consolidation Pressure.....	24
3.4 Compression, Re-compression and Swelling indices	26
3.5 Modulus of Compressibility (E_s).....	27
3.6 Laboratory Results and Discussion	30
Chapter 4: Constitutive model used for the numerical analysis.....	31
4.1 General.....	31
4.2 Basics of the Modified Drucker-Prager/cap plasticity model	31
4.3 Cap hardening.....	35
4.4 Flow Rule	39
Chapter 5: The Finite Element Method (FEM) results and discussion	41
5.1 General.....	41
5.2 Preprocessing.....	41
5.3 Postprocessing	44
5.4 Simulation of drained condition	44
5.5 Finite element results.....	45

Chapter 6: Conclusion and Recommendation	51
6.1 Conclusion	51
6.2 Recommendation	52
Reference	53
Appendix A	57
Appendix B	61
Appendix C	62
Appendix D	67

List of symbols

E_s	Modulus of Compressibility
E	Young's modulus
γ	Unit weight of the soil
FEM	Finite Element Method
P	Mean stress
σ_1	Deviator stress
σ_3	Cell pressure
ϕ'	Effective friction angle of the soil
c'	Effective cohesion of the soil
ϕ	Friction angle of the soil
c	Cohesion of the soil
Ψ	Dilatancy angle
e	Void ratio of the soil
e_0	Initial void ratio
G_s	Specific gravity
ν	poisson's ratio of the soil
σ	Normal stress
τ	Shear stress
d	Intersection of yield surface F_s with the t-axis
β	Slope of the yield surface F_s in the p-t plane
C_c	Compression index
C_s	Re-compression index

λ	Slope of normal consolidation line in e-lnp plane (re-loading)
κ	Slope of normal consolidation line in e-lnp plane (un-loading)
\mathcal{E}_v^p	Volumetric plastic strain
$\mathcal{E}_{v_0}^{pl}$	Initial cap position
R	Cap eccentricity
K	Flow stress ratio
α	Transition surface radius
P_b	Mean effective yield stress
LL	Liquid limit
PL	Plastic limit
SL	Shrinkage limit
PI	Plasticity index
w	Natural moisture content
ρ	Density
P_c	Pre-consolidation pressure
BM	Bole-Medhanialem
AG	Adisu-Gebeya
P_o	Over burden pressure
OCR	Over consolidation ratio
σ'	Effective normal stress
S'	Relative settlement
CU	Consolidated Undrained
UU	Unconsolidated Undrained

CD Consolidated Drained

MC Mohr-Coulomb

MDP Modified Drucker Prager

IL Incremental loading

CRS Constant rate of strain

BS British standard

FE Finite Element

ASTM American Society for Testing and Materials

List of figures

Fig. 2.1 Changes in soil states as a function of soil volume and water content (Budhu, 2000)..... 6

Fig. 2.2 Clay layer drained on the two faces (Das, B. M.,2008)..... 10

Fig. 2.3 Variation of u_i with depth (Das, B. M.,2008). 11

Fig.2.4 Variation of U_z with z/H and T_v (Das, B. M.,2008). 12

Fig. 2.5 Respective changes of U_{av} and T_v (Ndiaye, C., Fall, M., Ndiaye, M., Sangare, D., & Tall, A., 2014). 13

Fig. 2.6 One-dimensional consolidation test apparatus (Sam Helwany, 2007). 14

Fig. 2.7 Method of determining P_c by Casagrande method (Arrora, 2004). 15

Fig. 2.8 Typical loading-unloading curve to calculate compression and swelling indices (K.R.Arrora, 2004). 16

Fig. 2.9 Effective stress, σ'_v – axial strain, ϵ_1 relationships (Asad H., 2016)..... 21

Fig.2.10 Stress- Strain curve of Oedometer test and Plaxis simulation (R.J.Filipe,2001). 22

Fig.3.1 One dimensional consolidation test apparatus(AAiT Geotechnical laboratory). 24

Fig. 3.2 Void ratio versus log Pressure curves for red clay samples obtained from lab test..... 25

Fig. 3.3 Void ratio versus log Pressure curve for Adisu Gebeya Red clay 25

Fig. 3.4 Void ratio versus log Pressure curve for Kolfe area Red clay..... 26

Fig. 3.5 Effective normal stress vs Relative settlement of Red clay samples on linear scale 29

Fig.4.1 Modified Drucker-Prager/Cap model: yield surfaces in the p - t plane. (Adapted from Abaqus 2002). 32

Fig. 4.2 Projection of the modified cap yield surface on the π -plane (Abaqus,2002). 32

Fig. 4.3 Typical cap hardening behavior (Abaqus, 2002). 35

Fig. 4.4 Cap hardening curve for Adisu-Gebeya red clay; a) case-1 b)case-2 c) case-3 36

Fig. 4.5 Cap hardening curve for Kolfe area red clay; a) case-1 b) case-2 c) case-3..... 37

Simulation of Oedometer test using Finite Element Method

Fig. 4.6 Cap hardening curve for Rufael area red clay; a) case-1 b) case-2 c) case-3	38
Fig. 4.7 Flow potential of the modified cap model in the p-t plane (adopted from Abaqus manual, 2002).	39
Fig. 5.1 Symmetrical part and boundary condition of the sample.	43
Fig. 5.2 Descretised model.....	44
Fig. 5.3 FEM result for Adisu Gebeya red clay, case-1.....	46
Fig. 5.4 FEM result for Kolfe area red clay, case-1	47
Fig. 5.5 FEM result for Rufael area red clay, case-1	47
Fig. 5.6 Comparison of FEM result with the Oedometer test for Adisu-Gebeya red clay sample.	48
Fig. 5.7 Comparison of FEM result with the Oedometer test for Kolfe area red clay sample.....	48
Fig. 5.8 Comparison of FEM result with the Oedometer test for Rufael area red clay sample.	49

List of tables

Table 2.1 Ranges of properties of undisturbed Red clay soil from selected area of Addis Ababa. 7

Table 2.2 Consolidation properties of undisturbed red clay of Addis Ababa (Samuel T., 1989). 16

Table 2.3 Consolidation properties of red clay of Addis Ababa (Merihun L.,2010). 17

Table 2.4 Consolidation properties of Remolded red clay of Addis Ababa (Yodit M., 2012). 17

Table 2.5 Consolidation properties of Remolded red clay of Addis Ababa (Mustefa T., 2016). 18

Table 2.6 Data collected from previous studies for comparison (Mustefa T., 2016, Samuel T., 1989, Merihun L., 2010, Sorresa M., 2016, Hailemariam A., 2005 and Yodit M., 2012). 19

Table 3.1 Consolidation test result for red clay samples. 27

Table. 3.2 Effective normal stress,total compression and relative settlement of red clay samples. 29

Table 4.1 Cap hardening behaviour of Adisu Gebeya area red clay soils. 36

Table 4.2 Cap hardening behaviour of Kolfe area red clay soils. 37

Table 4.3 Cap hardening behaviour of Rufael area red clay soils. 38

Table 4.4 Average basic soil parameters for the Red clay soils for Adisu Gebeya , Rufael and Kolfe area. 40

..... 40

Table: 5.1 Comparison of relative settlement from laboratory and FEM results. 49

Chapter 1: Introduction

1.1 Background

When civil engineering structures rest on the ground, they induce stress on the underlying soil and the stress will be distributed in the soil mass. Depending on the engineering property, the response of the soil to the applied stress is different. As long as the applied stress does not exceed the load carrying capacity, the soil resists the applied load. It is also common to the applied stress to produce some deformation on the soil.

In a country like Ethiopia which is developing at high growth rate and which needs many construction works in the future, geotechnical investigation on the engineering properties of the supporting material is very essential.

Addis ababa is one of the fastest growing cities in the country and there are a huge volume of construction works. Red and Black clay soils are mainly found in the city. The soil ground of the city support different construction works like highrise buildings, roads, railway and stadiums that needs detail investigation of the ground. Therefore, engineering properties of these fine grained soils are important for design and construction of geotechnical structures. The compressibility behavior of fine grained soils such as clay is time-dependent. To characterize the above clay behavior one-dimensional conventional test which is Oedometer test is used. Oedometer test results have vital importance from geotechnical point of view, since settlement requirements usually control the design of foundations. The volume change characteristics of soils can be determined by means of the Oedometer tests in the laboratory. It is a conventional test, which is assumed to simulate the zero lateral strain condition on the specimen (M. Murat Monkul and Okan Onal, 2004).

The successful use of any numerical analysis in solving any geotechnical engineering problems depends on the constitutive model chosen to represent the actual material behavior. The constitutive model associated with a specific material has to describe the material evolution under external actions. There exist a large variety of models which have been recommended in recent years to represent the stress-strain and failure behavior of soils (Dipika Devi, 2013). Due to the complexity of real soil behavior, a single constitutive model that can describe all facets of behavior, with a reasonable number of input parameters, has not been achieved. Consequently, soil models are continuously developed and improved hence there are many soil models

available today, each of which has different advantages and limitations (Sushed Likitlersuang, 2003).

To investigate the engineering properties of these clay soils, many researches were done. Samuel T., 1989 and Merihun L., 2010, are some of the researchers which carried out on the engineering investigation of red clay soils of Addis Ababa. Simulation of Oedometer test is carried out by various researchers using different software's. Asad H., 2016 and R.J. Filipe, 2001 are some of the researchers which carried out simulation of Oedometer test using a finite element software Plaxis 2D. The FE software ANSYS was also used by P. Lenk, 2009 to simulate the scenario. Yuan, Yixing and Andrew J. Whittle, 2013 uses a finite element software ABAQUS to simulate the one-dimensional consolidation (Oedometer test).

1.2 Statement of the problem

Oedometer test is one of the common laboratory tests used to determine settlement parameters of fine-grained soils. To conduct this test, various incremental loads are applied to the sample with intermediate unloadings. This shows that the time it takes is one of the difficulties that engineers face in current geotechnical practices. So in this study the possibility of applying a finite element model to simulate the Oedometer test is examined in order to compare results with actual Oedometer tests and to use the model as one alternative for determining settlements, at least for preliminary design purposes.

1.3 Objective

1.3.1 General Objective

The general objective of this study is to simulate Oedometer test using finite element method for red clay soils from selected sites of Addis Ababa.

1.3.2 Specific Objectives

- To simulate Oedometer test using finite element method.
- To generate compressibility curves for the red clay soils under consideration.
- To determine the corresponding strain for the additional pressure due to the proposed structure on the given site.
- To determine Re-compression and Compression indices of the red clay soils under consideration.

1.4 Methodology

The work encompasses numerous methods and steps to carry out the task systematically. It entails literature survey, incorporation of available data, modeling the scenario and using of a FEM program.

First, a literature survey from different books, papers and thesis on the topic are done. This serves as a good platform to begin and frame the thesis properly. Then, all characteristics of clay at the specific location are collected as input data. These data may be collected as primary or secondary. Primary data such as modulus of elasticity, initial void ratio, pre-consolidation pressure, coefficient of compression and re-compression of the clay samples under consideration were determined from Oedometer tests of undisturbed samples in the laboratory.

Secondary data which contain all the above mentioned parameters and other remaining stress-strain behavior of the same soil have been collected from previously conducted and approved different studies on the area under consideration.

Afterwards, a realistic simulation of Oedometer test is conceptualized and a model of the soil sample is produced. This is the most important step in the thesis and serves as a bridge between the input data and the FEM analyses.

A FEM program-Abaqus version 6.13 is used to analyze the problem. Models are developed and simulated to perform 2D stress and settlement analysis. Based on the computation result analysis and interpretation was made. ASTM standard was used to carry out the one-dimensional consolidation of the clay samples collected from different selected area and for the data reviewed from literatures. Finally, conclusions and recommendations have been made on the basis of the result obtained.

1.5 Scope of the study

Undisturbed samples are used in this study for the simulation of Oedometer test using finite element method. Only loading part of the unloading-reloading procedures in the actual Oedometer test is simulated in this study.

With the attempts to achieve the above mentioned research objectives, samples were taken from Adisu-Gebeya and Kolfe area for the red clay. The major results and findings of this study are thus applicable for the particular areas listed above and other comparable clay soil conditions.

1.6 Organization of the thesis

This thesis work is divided in to six Chapters, each covering a specific topic of the research work. In the introductory Chapter background of the problem, objective of the research, methodology, scope of the investigation and organization of the thesis are presented. Literature review is undertaken in Chapter two. Laboratory tests and results goes to chapter three. Modeling of the incremental loading (IL) test using Abaqus is presented in Chapter four. Chapter five deals with Finite Element Method (FEM) results and discussion. The last Chapter, Chapter six, is devoted to conclusions and recommendations. Detailed test results are presented in the appendices.

Chapter 2: Literature review

2.1 Fundamental studies of clay soil behaviors

Clay is primarily composed of irregular arranged particles which have typical dimension of less than 2 μm . The particles are gathered in aggregates which are connected by bondings/links. These links are usually the smallest particles (Hansbo, 1975).

From engineering point of view, what distinguishes clay soil from other soil types is that they have a high degree of compressibility. It have the property of plasticity when it is mixed with water. Plasticity refers for the behaviour of a material that deforms in shape and keeps its deformation even after removal of the pressure that caused the material to deform (Vermeer & Neher, 1999).

Clay soil may contain clay minerals as well as non clay minerals. The non clay minerals that are found in clay are quartz, feldspar or mica. Clay minerals are mostly in the form of sheets; their thickness is relatively smaller than the width and length of the sheets, their surface area is larger than their volume. Consequently, the behavior of clay is governed by the surface forces. Soil behavior is attributed to the properties of clay minerals that are found in the specific soil. Therefore, it is vital to know the behavior of clay minerals for understanding the engineering behavior of fine grained soils (Merihun L., 2010).

2.2 Origin and mineralogical composition of redclay soils

According to Morin and Perry (1971), the red clay soils in Ethiopia are principally residual and derived from the weathering of volcanic rocks and they are developed in area where rainfall is plentiful and drainage is good, and they contain kaolinite and halloysite as their principal clay minerals. The red color of these clay soils indicates the presence of iron. The Ethiopian red clay is found to be acidic, which is similar to that of other tropical soils. The cation exchange capacity is from 30 to 77 milliequivalents per 100g. The Ethiopian red clay soils do not show wide range index properties as other tropical soils. They have also generally lower clay contents, liquid limits and plasticity indices (Morin, W.J., and Parry, W.T.,1971).Most Northern and Western parts of Addis Ababa is covered by red clay soils and a plenty of researches have been conducted on their engineering properties by different researchers.

2.3 Red clay soil distribution in Addis Ababa

Geotechnical drilling data and engineering geological map of Addis Ababa, reveals that red clay soils in Addis Ababa are dominantly underlain by basalts; basic (dark colored) igneous rock rich in iron and magnesium (Kebede T. and Tadesse H., 1990).

Geotechnical data from 1996 up to 2014 shows that, red clay soils in Addis Ababa are extensively distributed around Gulele sub-city, Burayu and part of Kolfe Keranyo. Some part of Addis Ketema and Arada sub-city are also covered with red clay soils (Lamesgin M., 2014).

Kokebe-Tsebah and British Embassy through Kotebe College of teachers Education are also parts of Addis Ababa city covered with red clay soil which are underlain by rhyolites. From these observations, it can be roughly generalized that red clay soils of Addis Ababa are dominantly derived from basalts and rhyolites (Lamesgin M., 2014).

2.4 Atterberg limits

If clay slurry is dried, the moisture content will gradually decrease, and the slurry will pass from a liquid state to a plastic state. With further drying, it will change to a semisolid state and finally to a solid state, as shown in Fig. 2.1. In 1911, Atterberg, a Swedish scientist, developed a method for describing the limit consistency of fine-grained soils on the basis of moisture content. These limits are the liquid limit, the plastic limit, and the shrinkage limit (Das, B.M, 1997).

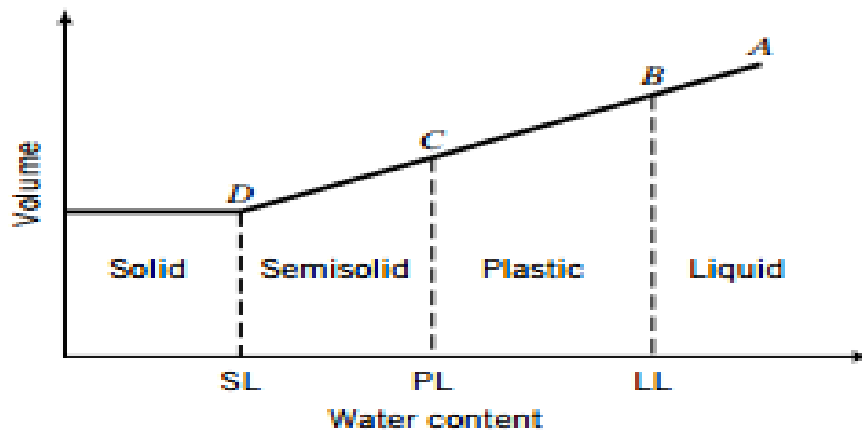


Fig. 2.1 Changes in soil states as a function of soil volume and water content (Budhu, 2000).

Simulation of Oedometer test using Finite Element Method

Litreture was reviewed from different researchs on the Atterberg limits (consistency) of Red clay of Addis Ababa as shown in Table 2.1. The Atterberg limits of the selected area for Red clay soils are presented according to Samuel T.,1989, Merihun L.,2010 and Jibril J.,2011.

Table 2.1 Ranges of properties of undisturbed Red clay soil from sellected area of Addis Ababa.

location (Sub-city)	Author	Specific site	Atterberg Limits			Specific gravity, G_s
			LL (%)	PL (%)	PI (%)	
Kolfe sub- city	Samuel T.	Kolfe	61-75	28-33	15-21	2.66-2.73
	Merihun L.	Kolfe pit 1	61	27	34	2.72
		Kolfe pit 2	71	33	38	2.73
	Jibril J.	Kalae	54.38	22.36	32.02	2.72
		Kolfe	68.97	30.89	38.08	2.77
		Traffic sefer	62.93	25.03	37.90	2.73
		Asko	69.38	32.43	36.95	2.69
Gulele sub- city	Samuel T.	Semen gebeya	59-72	24-31	33-47	2.7-2.77
		Rufael	56-66	27-34	29-41	2.66-2.74
	Merihun L.	Addis gebeya pit 1	63	28	35	2.71
		Addis gebeya pit 2	72	33	39	2.71
	Jibril J.	Addis gebeya	70.84	32.66	38.18	2.72
		Alem Tsehay dildy	60.50	23.57	36.93	2.73
		Atari	71.62	29.66	41.96	2.71
		Shgele	62.63	31.75	30.88	2.69
		Rufael	63.21	25.08	38.13	2.72
Semen mezegaja	56.87	23.03	33.84	2.68		

2.5 Consolidation of soils

When a load is applied on a standard soil mass, the entire load is first carried by the pore water, then due to the loading the water will drain out from the soil, transferring the loading to the soil skeleton. The differences between total applied stress and the pore pressure at any instant known as “effective stress” (Terzaghi, K.,1943). That is the same stress carried by the soil skeleton.

$$\sigma' = \sigma - u \dots \dots \dots (2.1)$$

In essence, the consolidation process is a gradual transfer of stress from the pore water to the soil skeleton.

2.5.1 Principle of consolidation

When a soil mass is subjected to a compressive force, like all other materials, its volume decreases. The property of the soil due to which a decrease in volume occurs under compressive forces is named as compressibility of soil. The compression of soils can occur due to one of the following reasons.

- a. Compression of solid particles and water in the voids.
- b. Compression and expulsion of air in the voids.
- c. Expulsion of water in the voids.

2.5.2 Consolidation theory

Terzaghi made assumptions on the process of consolidation and designed the first consolidation apparatus for consolidation test. Many of the geotechnical engineers use the Terzaghi theory to solve various types of problem related to soils. The classical one-dimensional consolidation Terzaghi theory is based on the following assumptions (Terzaghi, K.,1943).

- a) Homogeneous clay layer.
- b) Fully saturated clay layer.
- c) Compressibility of soil grains and water is negligible.
- d) Deformation of soil occurs only in the direction of the load application.
- e) Darcy’s law is valid.

f) Flow is in one direction only

g) The coefficient of permeability is constant within the layer.

In case of simple one-dimensional consolidation of clay layer that is subjected to a uniform load the following equation of Terzaghi is proposed.

$$\frac{\partial u}{\partial t} = \frac{k}{\gamma_w m_v} \frac{\partial^2 u}{\partial z^2} \dots\dots\dots(2.2)$$

where , u = excess pore water pressure at time t, at a given point.

z = vertical height of that point.

k = coefficient of permeability of the clay.

m_v = coefficient of volume compressibility of the clay.

γ_w = unit weight of water.

Defining the coefficient of consolidation, C_v as:

$$C_v = \frac{k}{\gamma_w m_v} \dots\dots\dots(2.3)$$

Equation 2.2 becomes,

$$\frac{\partial u}{\partial t} = C_v \frac{\partial^2 u}{\partial z^2} \dots\dots\dots(2.4)$$

Equation (2.4) is the basic differential equation of Terzaghi's consolidation theory and can be solved by combining two boundary conditions and initial condition.

- Boundary conditions (for all time t)
 - On the surface of the layer, z = 0, we have: u (0, t)= 0
 - At the bottom of the layer, z = 2H, then:u (2H, t)= 0
- Initial condition (for t = 0)
 - U (z,0)= Δσ_v except for z = 0 and z = 2H

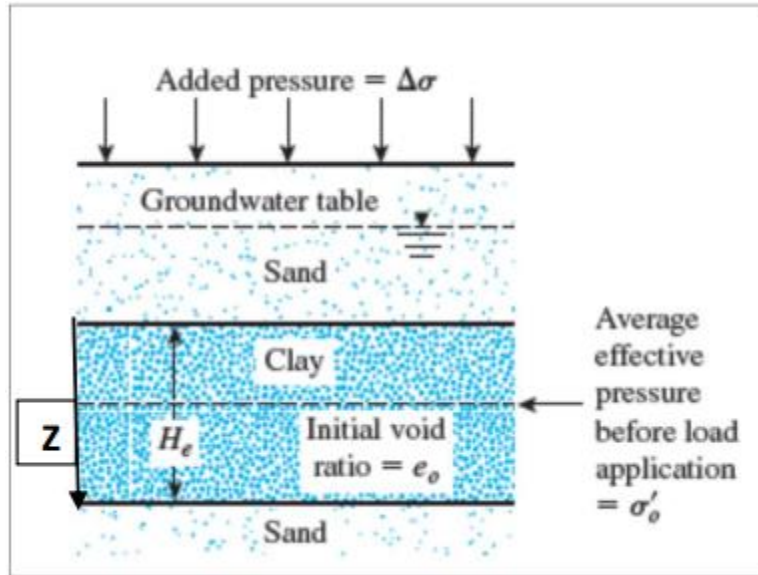


Fig. 2.2 Clay layer drained on the two faces (Das, B. M.,2008).

The analytical solution of equation in conjunction with the conditions is obtained through Fourier series transformation function. The general solution of Terzaghi equation (Alemayehu T. &Mesfin L., 1999) is

$$u = \sum_{n=1}^{n=\infty} \left(\frac{1}{H} \int_0^{2H} u_i \sin \frac{n\pi z}{2H} dz \right) \sin \frac{n\pi z}{2H} \exp \left(\frac{-n^2 \pi^2 c_v t}{4h^2} \right) \dots \dots \dots (2.5)$$

The expression of $\left(\frac{c_v t}{h^2}\right)$ is a dimensionless number and replaced by a time factor, T_v as

$$T_v = \frac{c_v t}{h^2} \dots \dots \dots (2.6)$$

By substituting Equation 2.6 into the general solution equation, the simplified equation becomes,

$$u = \sum_{n=1}^{n=\infty} \left(\frac{1}{H} \int_0^{2H} u_i \sin \frac{n\pi z}{2H} dz \right) \sin \frac{n\pi z}{2H} \exp \left(\frac{-n^2 \pi^2 T_v}{4} \right) \dots \dots \dots (2.7)$$

where, u = pore water pressure

u_i = initial pore water pressure

H = height of specimen

T_v = time factor

z = vertical height (top to bottom of specimen)

So far, no assumptions have been made regarding the variation of u_i with the depth of the clay layer. Several possible types of variation for u_i are shown in Fig. 2.3.

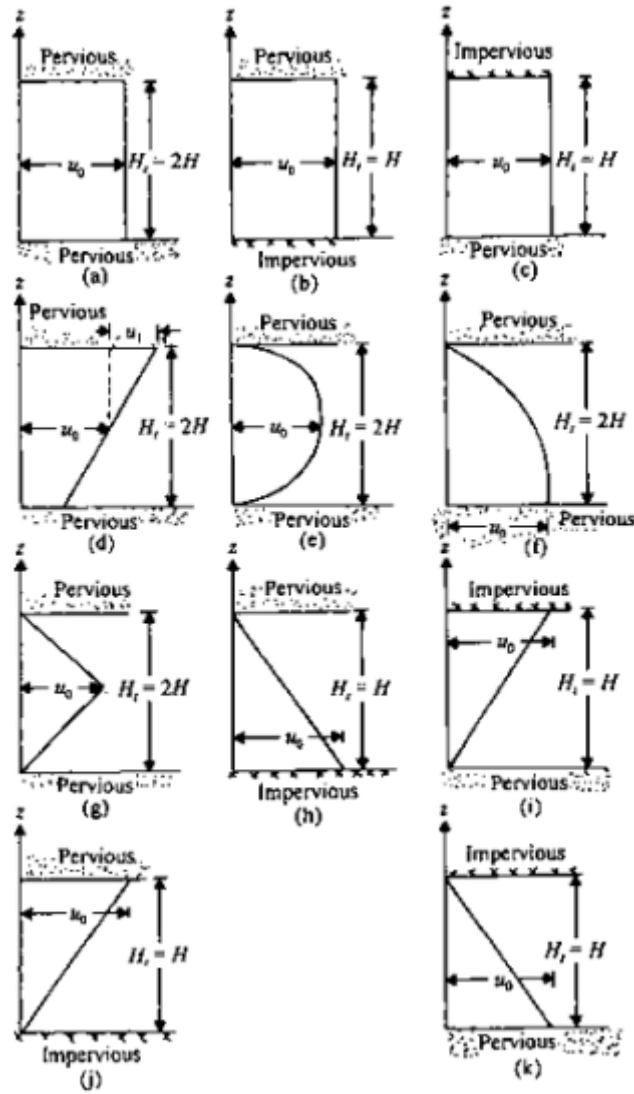


Fig. 2.3 Variation of u_i with depth (Das, B. M.,2008).

At any stage during the consolidation process, transfer of stress from the pore water to soil skeleton are known as degree of consolidation, U . This process is expressed in percentage. Degree of consolidation, U at time t can be calculated by Equation 2.8.

At a given time the degree of consolidation at any depth z is defined as

$$U_z = \frac{\text{excess pore water pressure dissipated}}{\text{initial excess pore water pressure}}$$

$$U_z = \frac{u_i - u}{u_i} = 1 - \frac{u}{u_i} = \frac{\Delta\sigma'}{u_i} = \frac{\Delta\sigma'}{u_o} \dots\dots\dots(2.8)$$

From Equations 2.7 and 2.8 (Das, B. M.,2008).

$$U_z = 1 - \sum_{m=0}^{m=\infty} \frac{2}{m} \sin \frac{Mz}{H} \exp(-M^2 T_v) \dots\dots\dots(2.9)$$

Where $M=(2m+1)\pi/2$

Figure 2.3 shows the variation of U_z with depth for various values of the non-dimensional time factor T_v ;

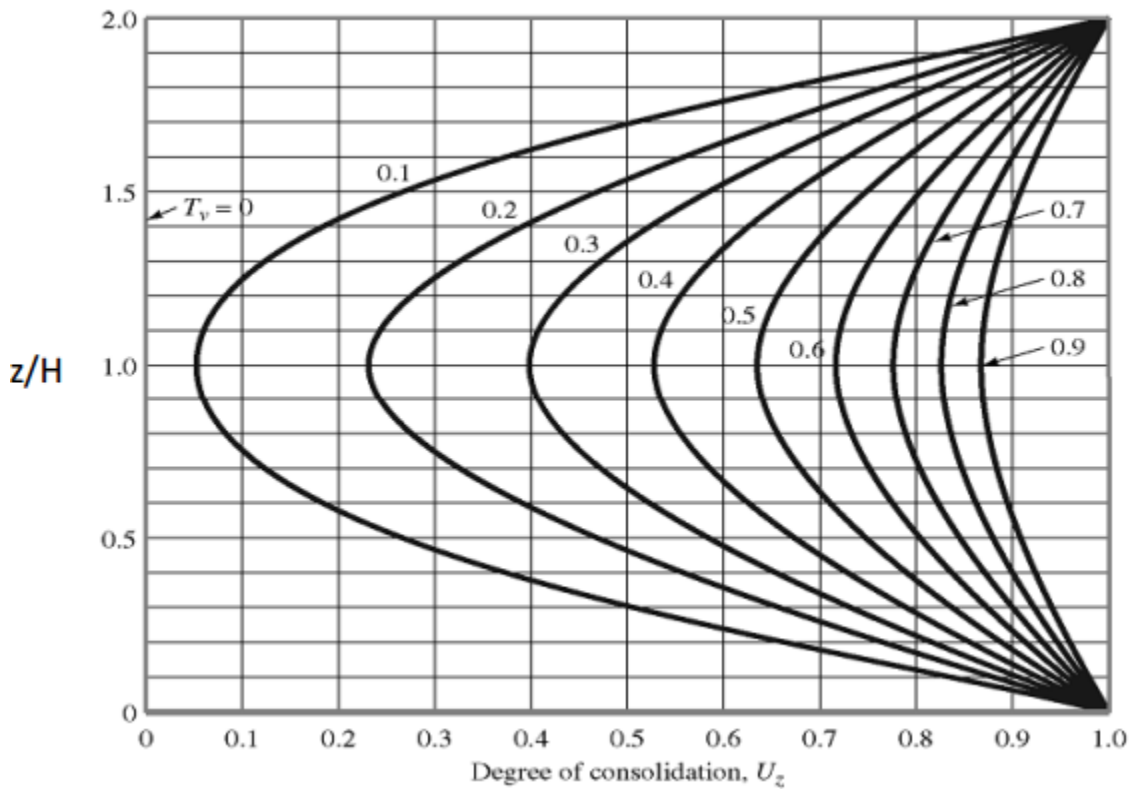


Fig.2.4 Variation of U_z with z/H and T_v (Das, B. M.,2008).

The average degree of consolidation is also the ratio of consolidation settlement at any time to maximum consolidation settlement. Average degree of consolidation (U) for the entire depth of the clay layer at any time, t is (Alemayehu T. & Mesfin L.,1999).

$$U_{av} = 1 - \sum_{m=0}^{m=\infty} \frac{2}{M^2} \exp(-M^2 T_v) \dots \dots \dots (2.10)$$

Hence the representation of the function U_{av} vs (T_v) and the inverse function T_v vs (U_{av}) are given in Fig.2.4.

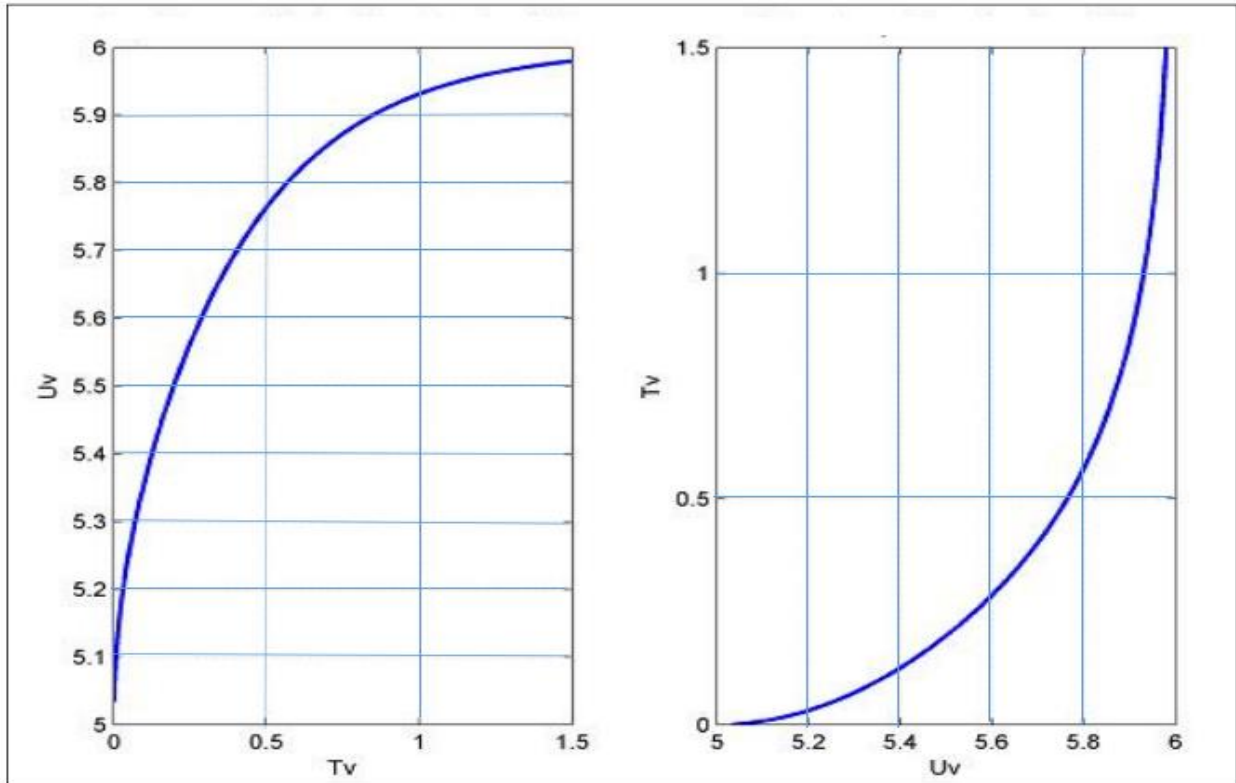


Fig. 2.5 Respective changes of U_{av} and T_v (Ndiaye, C., Fall, M., Ndiaye, M., Sangare, D., & Tall, A., 2014).

2.5.3 One-Dimensional consolidation test

The usual way to conduct a one-dimensional consolidation test is to confine a soil sample in a fixed stiff metal ring with the sample loaded along the vertical axis of the ring. Compression of solid particles and water in the voids is very small and its effects become negligible due to their compressibility property under stress application. Compression due to expulsion of air is also not relevant due to its quickly expelled property as soon as the load is applied. Therefore, the compression of soil is mainly caused due to the third factor which is expulsion of water in the voids (K.R. Arora, 2004).

Consolidation of a saturated soil occurs due to expulsion of water under static, sustained load. The consolidation characteristics of soils are required to predict the magnitude and the rate of settlement.

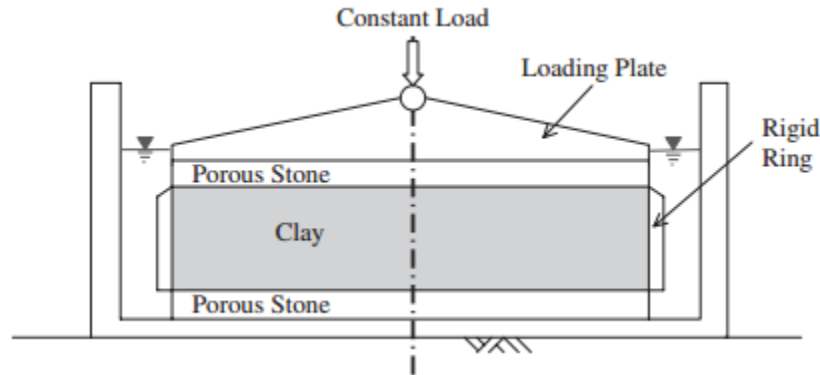


Fig. 2.6 One-dimensional consolidation test apparatus (Sam Helwany, 2007).

The one dimensional consolidation test is carried out to study the compressibility of the soil using the apparatus called Oedometer. The consolidation parameters of a soil are compression index (C_c) and coefficient of consolidation (C_v). The compression index relates to how much consolidation or settlement will take place while the coefficient of consolidation relates to the time of consolidation to take place. Soil samples having diameter of 50mm and height of 20mm were loaded from 25 kPa to 1600kPa by doubling the loading. Compression were recorded from the dial guage at time intervals of: 0,0.25,0.5,1,2, and 4.....1440 minutes (Hansbo, 1975).

When attempting to investigate the compressibility of soils, the oedometer test is the most common choice. The tests can be performed as either incrementally loaded tests or as constant rate of strain tests (Larsson, 1986).

2.5.2 Incremental Loading (IL) test

The incremental loading Oedometer test is commonly used worldwide to determine the compression properties of fine grained soils. IL test procedure consists of several incremental loading steps, for instance, 50, 100, 200, 400, 800,1600 kPa. Each step is allowed to sustain for 24 hours until the next load is applied (Sällfors, 1975).

2.5.3 Constant rate of strain test (CRS)

In CRS test, the sample is deformed with a constant speed (the standard test speed in Sweden is 0.0024mm/min, i.e. 0.72%/h). The applied load, deformation and the pore water pressure are continuously measured during the test (Par Gustafsson,2011).

2.5.4 Pre-Consolidation pressure (P_c)

A soil may have been pre-consolidated during the past geologic events by the weight of an ice which has melted away, structural loads which no longer exist or/and due to other geologic overburden. For example, thick layers of overburden soil may have been eroded or excavated away or heavy structures may have been torn down. Its practical significance of the pre-consolidation pressure appears during settlement calculation of structures (Jumikis A.R., 1984).

There are a few graphical methods employed to determine P_c based on consolidation laboratory test data. Among these methods, the earliest and most widely used method was the one proposed by Casagrande (1936). The method involves locating the point of maximum curvature, B , on the laboratory e - $\log p$ curve of an undisturbed sample as shown in Fig 2.7. From B , a tangent is drawn to the curve and a horizontal line is also constructed. The angle between these two lines is then bisected. The abscissa of the point of intersection of this bisector with the upward extension of the inclined straight part corresponds to the preconsolidation pressure, P_c (Murthy, V.N.S., 1990).

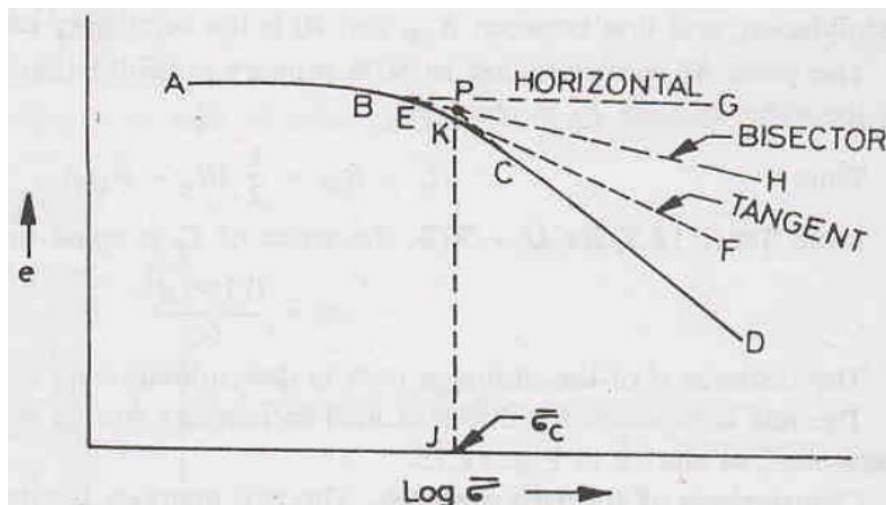


Fig. 2.7 Method of determining P_c by Casagrande method (Arrora, 2004).

2.5.5 Compression and Re-compression indices

Compression index, C_c is equal to the slope of the linear portion of e vs $\log p$ curve in loading case. Similarly, re-compression index, C_r is the slope of the curve obtained during reloading. C_c and C_r are useful for determination of the settlement in the field.

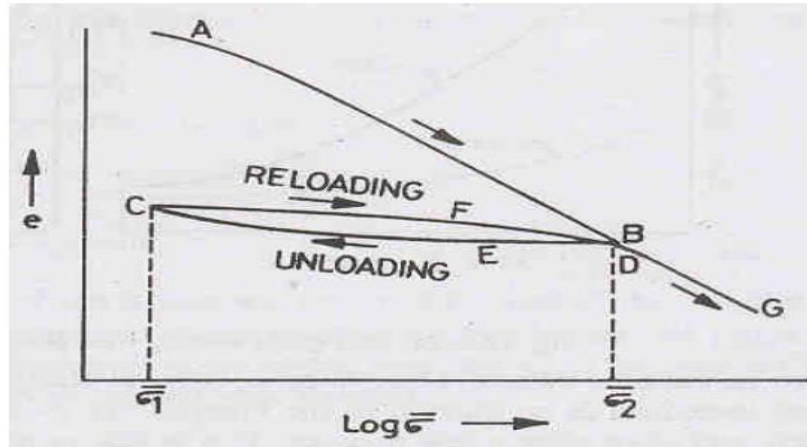


Fig. 2.8 Typical loading-unloading curve to calculate compression and swelling indices (K.R.Arrora, 2004).

2.5.6 Consolidation properties of Addis Ababa red clay

It was shown that the predominant mineral of Addis Ababa red clay is kaolinite and halloysite (Samuel T, 1989). Studies on the general characteristics of Addis Ababa red clays have been carried out to date by many researchers. The geotechnical properties of Addis Ababa red clay have been reported by (Samuel T., 1989) and other researchers. The laboratory measured soil compressibility and compression characteristics are investigated by different researchers.

The following Tables (Table 2.2 - 2.5) show consolidation properties of Addis Ababa red clay according to researchers.

Table 2.2 Consolidation properties of undisturbed red clay of Addis Ababa (Samuel T., 1989).

Location	Depth, m	$C_v(\text{avg.})(10^{-4}\text{cm}^2/\text{sec})$	C_c	P_c
Kolfe	3	19.63	0.136	200
Semen-mazegaja	1.5	17.665	0.146	180
Rufael	1.5	18.975	0.153	215

Simulation of Oedometer test using Finite Element Method

Table 2.3 Consolidation properties of red clay of Addis Ababa (Merihun L.,2010).

Location	Depth (m)	$C_v(\text{avg.})(10^{-4}\text{cm}^2/\text{sec})$		C_c		P_c	
		UND.	REM.	UND.	REM.	UND.	REM.
Kolfe pit-1	2.5	46.02	25.22	0.147	0.175	320	220
Kolfe pit-2	2.5	46.3	23.37	0.196	0.24	380	180
Adisu Gebeya pit-1	2.5	46.36	16.99	0.152	0.204	380	140
Adisu Gebeya pit-2	2.5	40.8	16.725	0.178	0.236	280	100

where UND. = Undisturbed Soil Sample, REM. = Remolded Soil Sample

Table 2.4 Consolidation properties of Remolded red clay of Addis Ababa (Yodit M., 2012).

Location	Depth, m	C_c	P_c
Kolfe pit-1	1.5	0.199	75
Kolfe pit-2	3	0.186	
Adisu Gebeya pit-1	1.5	0.199	60
Adisu Gebeya pit-2	3	0.191	
Atena tera pit-1	1.5	0.203	260
Atena tera pit-2	3	0.227	
Athari pit-1	1.5	0.209	70
Athari pit-2	3	0.225	
Awelya pit-1	1.5	0.176	100
Awelya pit-2	3	0.180	
Shegole pit-1	1.5	0.209	160
Shegole pit-2	3	0.180	

Table 2.5 Consolidation properties of Remolded red clay of Addis Ababa (Mustefa T., 2016).

Soil sample	Compression index , C_c			C_s	C_c	Pre-consolidation pressure
	From $e-\log\sigma'_v$ Plot graph	From emperical formula				
		Terzaghi and peck	Nagaraj and Murthy			
Kolfe pit-1	0.105	0.450	0.366	0.020	0.186	360
Kolfe pit-2	0.125	0.567	0.469	0.022	0.179	198
Adisu Gebeya Pit-1	0.122	0.477	0.406	0.034	0.276	300
Adisu Gebeya Pit-2	0.123	0.513	0.427	0.022	0.180	290
Rufael pit-1	0.124	0.450	0.378	0.018	0.143	300
Rufael pit-1	0.103	0.549	0.451	0.017	0.168	320

All researchers used conventional incremental load (CIL) consolidation test to describe the consolidation properties of Addis Ababa red clay, which is common test in our country.

The input parameters such as modulus of elasticity, angle of internal friction, cohesion, void ratio, pre-consolidation pressure, specific gravity, unit weight, coefficient of compressibility and coefficient of expansion for the Cap Plasticity model were collected from previous studies as shown in Table 2.6 and the average value of these parameters were used during the simulation of Oedometer test using the finite element software Abaqus.

Simulation of Oedometer test using Finite Element Method

Table 2.6 Data collected from previous studies for comparison (Mustefa T., 2016, Samuel T., 1989, Merihun L., 2010, Sorresa M., 2016, Hailemariam A., 2005 and Yodit M., 2012).

Location	Parameters	Authors						Average parameters
		Mustefa T.	Samuel T.	Merihun L.	Sorresa M.	Hailemariam A.	Yodit M.	
Adisu Gebeya red clay soil	E	11,216.32	-	10,243.86	-	12,206.07	10,897.24	11,140.87
	C _c	0.123	-	0.22	-	0.124	0.219	0.172
	C _s	0.038	-	0.029	-	0.0196	0.0245	0.0278
	e _o	0.832	-	0.852	-	0.892	0.876	0.863
	P _c	290	-	120	-	235	198	210
	G _s	2.72	-	2.72	-	2.76	2.73	2.73
	γ	18.9	-	19.1	-	19.2	19.3	19.13
	Ø	24	-	26	-	29	27	26.5
	C	21	-	23	-	23	25	23
Kolfe area red clay soil	E	10,687.16	9958.2	11,578.91	11,354.18	9827.26	10,615.38	10,670.18
	C _c	0.125	0.136	0.208	0.195	0.108	0.189	0.16
	C _s	0.018	0.015	0.022	0.0285	0.015	0.0179	0.0194
	e _o	0.795	0.959	0.793	0.823	0.814	0.921	0.851
	P _c	198	200	200	380	230	235	240.5
	G _s	2.74	2.69	2.7	2.74	2.74	2.70	2.72
	γ	18.2	18.5	18.5	19.13	18.5	18.8	18.61
	Ø	21.5	21.5	28	27.5	26	25	25
	C	25	27	26	24.5	28	29	26.58
Rufael area red clay soil	E	9876.73	-	9946.77	-	10,648.48	10,376.45	10,212.11
	C _c	0.103	-	0.198	-	0.196	0.196	0.173
	C _s	0.018	-	0.0215	-	0.023	0.0184	0.0202
	e _o	0.742	-	0.836	-	1.04	0.893	0.878
	P _c	320	-	170	-	270	240	250
	G _s	2.71	-	2.72	-	2.73	2.69	2.71
	γ	17.8	-	17.9	-	18.2	18.3	18.05
	Ø	25	-	26	-	27	26	26
	C	22	-	23	-	25	24	23.5

2.6 Constitutive models

2.6.1 General

Over the last few decades, the developments in the fields of constitutive modeling and numerical methods have given engineers a robust tool which allows analyzing soil behavior by means of computer simulations. Complex soil behavior can be represented by mathematical models which are governed by a set of material properties (Mohammed Fattah & Bestun J Shwan, 2011).

The constitutive soil models can be divided into two groups: elastic and elasto-plastic models. The simple linear isotropic elastic models, which require only two material parameters, do not simulate any of important behavior of real soil.

The elastic perfectly plastic soil models which requires an extra input parameter than elastic models better to simulate some of the important behavior of clay soils (Sushed Likitlersuang, 2003). But experimental evidence indicates that the plastic deformation in soils starts from the early stages of loading and to capture such a behavior in a constitutive model the typical elasto-perfect plastic models are not adequate. Hence, to simulate such behavior constitutive models that utilize a hardening law after initial yielding are required (Ahmed B., 2006).

2.7 Related studies

Different researchers are developing a finite element model to simulate 1D consolidation (Oedometer test) using various constitutive soil models.

Asad H. (2016), had carried out numerical simulation of one-dimensional Compression (Oedometer test) on cohesionless specimens for both dense and loose sand in the geotechnical laboratories of Wasit University. During his simulation, Plaxis 2D finite element software was used to simulate the consolidation phenomenon in Oedometer test. He considered a rectangular axisymmetric model having dimensions similar to the samples used in the laboratory and very fine mesh was used during the simulation. Hardening soil model was used to consider both the shear hardening due to the deviatoric loading & the compression hardening due to primary compression in Oedometer loading. Irreversible strain is also taken into account during the simulation process (Schanz, 1998).The results of both laboratory test (one-dimensional compression test) and the finite element analysis were plotted in e - $\log \sigma'_1$ space as well as stress-strain relationship. After the application of the incremental loads in Plaxis, he obtained similar results with what should have to be in the Oedometer test.

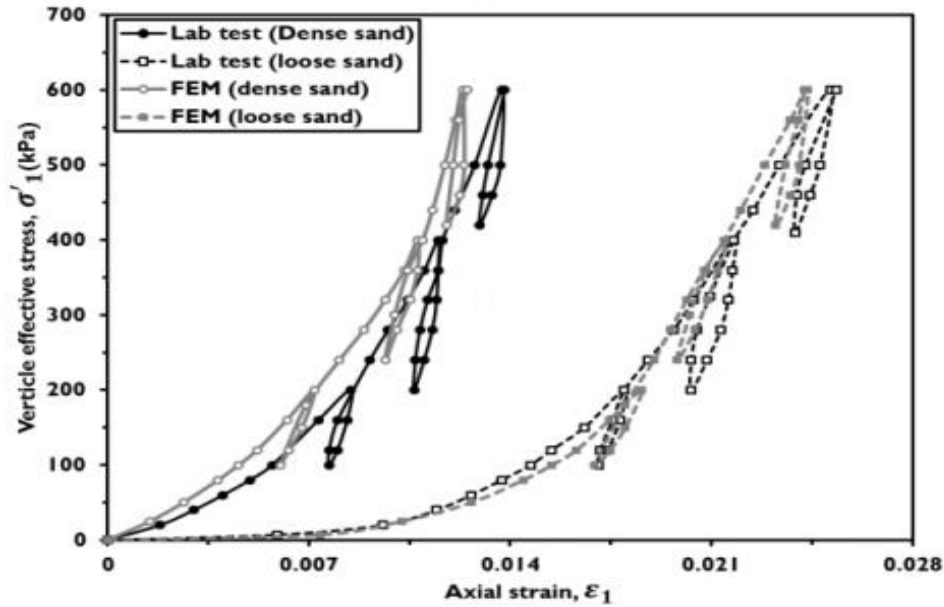


Fig. 2.9 Effective stress, σ'_v – axial strain, ϵ_1 relationships (Asad H., 2016).

To support his study, Oedometer test results agree with typical finite element analysis results found for soils such as in Knappett and Craig (2012) for e - $\log \sigma'_1$ space and Benz(2008) for σ'_1 - ϵ_1 space were reviewed. It is also observed that, the finite element analysis results were found to be very slightly under predicting the stiffness in the loose state at low stress level where as it was tiny over predicting for higher stress level. Finally, he concluded that, great prediction was observed in the effective vertical stress-axial strain relationship in both the loose and dense state. The one-dimensional consolidation test using finite element analysis primarily can be used in the initial stage of footing design in cohesionless soil.

Lenk (2009) modelled Oedometer test in 3D using the finite element software ANSYS. A comparison of the experimental measurements and finite element analysis results was made after the scenario has been modelled using the appropriate constitutive model and input parameters. As a result, the FE analysis results were found consistent with the experimental Oedometer test results. He also observed that, significant results were obtained concerning the vertical deformations over time. He concluded that, the time-dependent settlement of the foundations of buildings can be calculated with the proper application of FEM model to geological subsoil condition.

Numerical analysis of one-dimensional consolidation test was carried out by Yuan, Yixing and Whittle (2013), to simulate the incremental Oedometer tests using Soft Soil Creep (SSC) and Isotache models. The simulations were conducted on normally consolidated Yokohama clay soil. They used the SSC model to incorporate a time-dependent state variable to estimate viscoplastic deformation. Effects of specimen thickness and the phenomenon of pore water pressure increases at the beginning of consolidation are discussed in detail under their study. The results they obtained from laboratory tests and finite element analysis using both viscoplastic models are very consistent. Finally, they concluded that, application of viscoplastic models (such as SSC) in the finite element method are important for predicting consolidation at field scale.

Filipe (2001) had studied the compression phenomenon using Oedometer test on a saturated cohesive specimens in order to assess the deformations along the loading time and according to various loads. A finite element software Plaxis 2D was used to simulate the scenario. The model was designed by an extract with 34 mm high and 63 mm wide, just like samples tested in the laboratory. The boundary conditions imposed on the specimen was considered mobile supports laterally, which only allow vertical displacements. On the bottom side, the model considers fixed supports which prevent displacement in any direction. Triangular elements with 15 nodes are used in the finite element mesh he adopted.

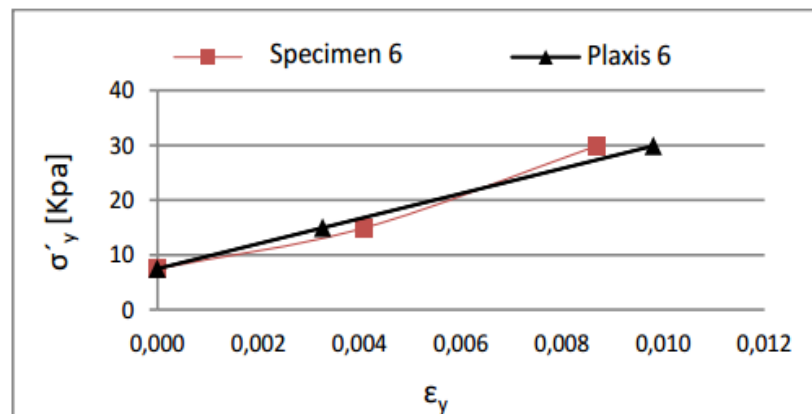


Fig.2.10 Stress- Strain curve of Oedometer test and Plaxis simulation (R.J.Filipe,2001).

Finally, he observed good agreements between the finite element analysis results and the one-dimensional consolidation test results (Fig. 2.10).

Chapter 3: One- Dimensional Consolidation (Oedometer) tests and results

3.1 General

In this chapter, One-dimensional consolidation, which is the most commonly applied soil test to determine stiffness and compressibility parameters of cohesive specimens in the laboratory is firstly described, including the different instruments and their testing methods. Then, evaluation of the important soil parameters required by the model are discussed.

3.2 One - Dimensional Consolidation (Oedometer) test

When a saturated clay-water system is subjected to an external pressure, the pressure applied is initially taken by the water in the pores resulting thereby in an excess pore water pressure. If drainage is permitted, the resulting hydraulic gradients initiate a flow of water out of the clay mass and the mass begins to compress. A portion of the applied stress is transferred to the soil skeleton, which in turn causes a reduction in the excess pore pressure. This process, involving a gradual compression occurring simultaneously with a flow of water out of the mass and with a gradual transfer of the applied pressure from the pore water to the mineral skeleton (Arrora, 2004).

In an Oedometer test the sample is enclosed by a ring that is connected to a bottom plate. In order to reduce the friction inside the ring, it is applied with a silicon paste or the ring itself could be made of Teflon. The standard inner diameter and the height of the sample are 50 mm and 20 mm respectively (Hansbo, 1975). There are porous filter stones located both on the top and bottom, which allow the sample to be two sided drained. The top one is connected to a stamp where the load is added vertically as shown in Figure 3.1. Here under this study the incrementally loaded test was used.

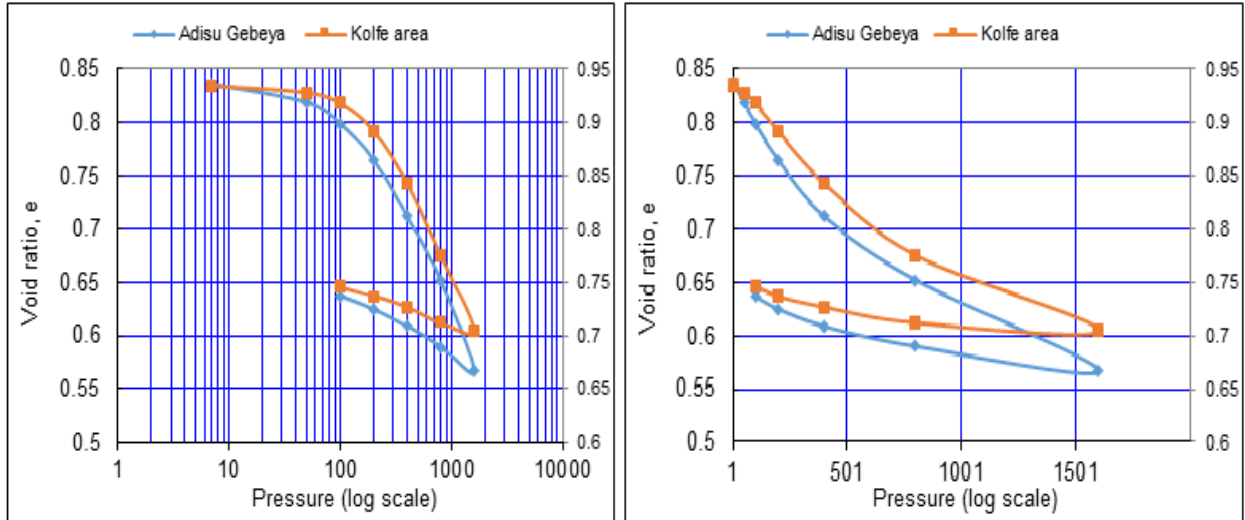
Figure 3.1 illustrates, the incremental loading Oedometer apparatus used at the Geotechnical laboratory of AAiT. To carry out this test undisturbed samples were collected from Addisu Gebeya and Kolfe area from a depth of 3 m and 2.5 m respectively. Diameter of 50 mm soil samples having height of 20 mm were loaded from 50 kPa to 1600 kPa by doubling the loading. For each loading the compression of the sample were recorded from the dial guage at time intervals of 0.15, 0.25, 0.5, 1, 2, 4,.....1444 minute for twenty-four hours. Unloading was also done by steps to examine the unloading behaviour of the samples (Appendix A).



Fig.3.1 One dimensional consolidation test apparatus(AAiT Geotechnical laboratory).

3.3 Pre-consolidation Pressure

The pre-consolidation pressure, P_c for each of the soil sample was determined from the Void ratio versus log pressure curve using Casagrande's method as it is discussed in Buduhu, 2007, and are presented as shown in Table 3.1. These results indicate that, all the soil samples which were collected from the selected sites are over-consolidated in their natural state. Figure 3.2 show that void ratio versus pressure curves in logarithmic and natural scale for the Red clay samples collectd from Adisu Gebeya and Kolfe are (detailed calculation is attached in Appendix B).



a) log scale

b) linear scale

Fig. 3.2 Void ratio versus log Pressure curves for red clay samples obtained from lab test.

The pre-consolidation, P_c value of the specimens can be determined using both the approximate (simplified) and Casagrande's method. In this study, P_c value for both the red clay samples collected from Adisu-Gebeya and Kolfe area were computed using Casagrande's method as shown in Figure 3.3 and 3.4.

Determination of P_c using Casagrande's method for Adisu Gebeya Red clay sample

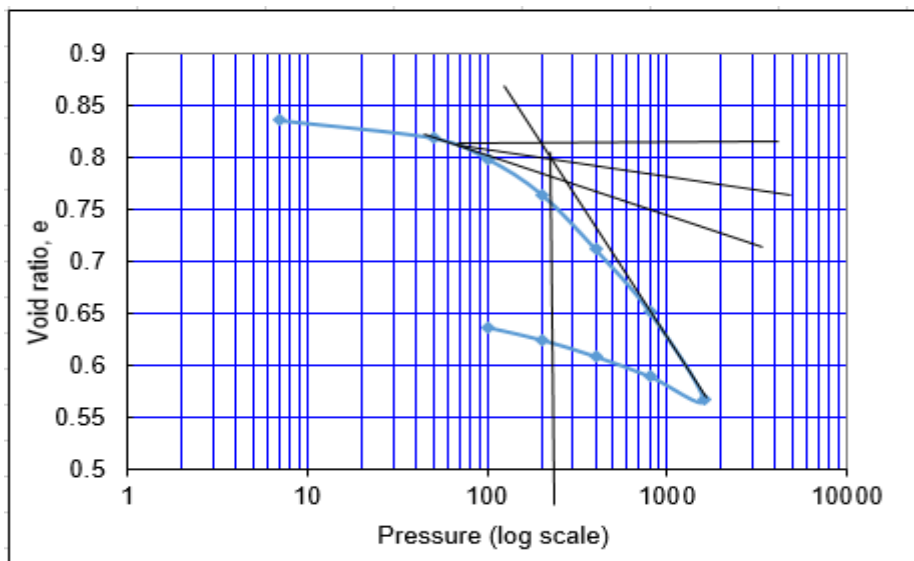


Fig. 3.3 Void ratio versus log Pressure curve for Adisu Gebeya Red clay

Determination of P_c using Casagrande's method for Kolfe area Red clay sample

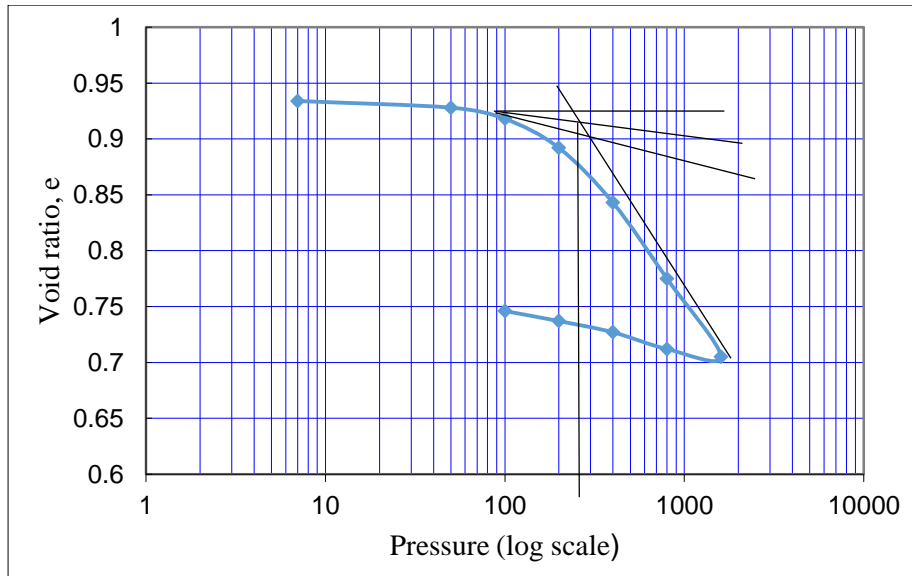


Fig. 3.4 Void ratio versus log Pressure curve for Kolfe area Red clay.

3.4 Compression, Re-compression and Swelling indices

The compression index, C_c is equal to the slope of the linear portion of the Void ratio versus log Pressure and expansion or swelling index, C_s is the slope of the Void ratio versus log Pressure curve obtained during unloading. Re-compression index, C_r is obtained from the slope of the Void ratio versus log Pressure curve with in the effective overburden pressure to the point of Pre-consolidation pressure, P_c . The values of compression index, C_c , Re-compression index, C_r and expansion or swelling index, C_s of the red clay samples are tabulated as shown in Table 3.1.

Table 3.1 Consolidation test result for red clay samples.

Location	Depth of sampling(m)	Unit weight, Y_t (kN/m ³)	Pressure (P) kN/m ²	Void ratio (e)	Swelling index (C_s)	Re-Compression index (C_r)	Compression index (C_c)	Over burden pressure(P_o) kN/m ²	Preconsolidation pressure (P_c), kN/m ²	OCR, P_c/P_o
Addisu Gebeya	3	19.2	7	0.826	0.055	0.031	0.215	76.8	220	2.86
			50	0.809						
			100	0.796						
			200	0.745						
			400	0.692						
			800	0.632						
			1600	0.567						
Kolfe area	2.5	18.6	7	0.934	0.059	0.033	0.23	46.5	260	5.6
			50	0.928						
			100	0.912						
			200	0.892						
			400	0.833						
			800	0.775						
			1600	0.705						

3.5 Modulus of Compressibility (E_s)

The modulus of compressibility, E_s is a basic parameter that describes the compressibility behavior of soils and governs the results of settlement related problems. The use of a practical and reasonable E_s values representing the in situ conditions is of great importance in finite element analysis for better simulation of the actual condition of the soil.

According to Alemayehu T. and Mesfin L.,1999, the compressibility curve obtained from the consolidation test may be expressed with sufficient accuracy by the equation:

$$E_s = \frac{\partial \sigma'}{\partial s'} = v(\sigma')^w \dots\dots\dots(3.1)$$

In the above eq. s' is the relative settlement, v and w are coefficients where v has a unit of kPa. It depends on the void ratio, moisture content and consistency of the sample. It could have values ranging from 50 to 30,000 kPa. The coefficient w is a dimensionless quantity which depends on the soil type. It could have values ranging from 0 to 1. The tangent of the compressibility curve, which is a function of σ' gives the modulus of compressibility, E_s .

From eq. (3.1)

$$\frac{\partial s'}{\partial \sigma'} = \frac{1}{v(\sigma')^w} \dots \dots \dots (3.2)$$

$$\partial s' = \frac{(\sigma')^{-w}}{v} \partial \sigma' \dots \dots \dots (3.3)$$

$$s' = \frac{1}{v} \int (\sigma')^{-w} \partial \sigma \dots \dots \dots (3.4)$$

Case #1: for w differs from 1

$$s' = \frac{1}{v(1-w)} (\sigma')^{1-w} + c \dots \dots \dots (3.5)$$

Defining $a = \frac{1}{v(1-w)}$ and $k = 1-w$, eq.(4.5) becomes

$$s' = a(\sigma')^k + c \dots \dots \dots (3.6)$$

Case #2: for w equals to 1

$$\frac{\partial s'}{\partial \sigma'} = \frac{1}{v\sigma} \dots \dots \dots (3.7)$$

$$s' = \frac{1}{v} \ln \sigma' + c \dots \dots \dots (3.8)$$

Where: c is constant of integration

As it is observed from Fig. 3.6 , when σ' equal to zero, s' will also be zero. Therefore eq.(3.6) becomes:

$$s' = a(\sigma')^k \dots \dots \dots (3.9)$$

The same is true for eq. (3.8) and taking common logarithmic of eq. (3.9) it becomes:

$$\log S' = k \log \sigma' + \log a \dots \dots \dots (3.10)$$

The values used to plot Eq. (3.10) are tabulated in Table 3.2 for the Red clay samples.

Simulation of Oedometer test using Finite Element Method

Table. 3.2 Effective normal stress, total compression and relative settlement of red clay samples.

Location	Depth (m)	Effective normal stress, σ' , (kN/m ²)	Total compression, ΔH , (mm)	Relative settlement, $s' = \Delta H/H$	Modulus of compressibility, E_s (MPa)
Adis-Gebeya	3	7	0.055	0.00275	10.4
		50	0.245	0.0122	
		100	0.386	0.0193	
		200	0.935	0.04675	
		400	1.519	0.07595	
		800	2.169	0.10845	
		1600	2.885	0.14425	
Kolfe	2.5	7	0.065	0.00325	9.6
		50	0.268	0.0134	
		100	0.435	0.02175	
		200	1.045	0.05225	
		400	1.642	0.0821	
		800	2.372	0.1186	
		1600	3.038	0.1519	

The effective normal stress versus relative settlement of both the red clay samples collected from Adisu-Gebeya and Kolfe areas are plotted as shown below in Figure 3.5.

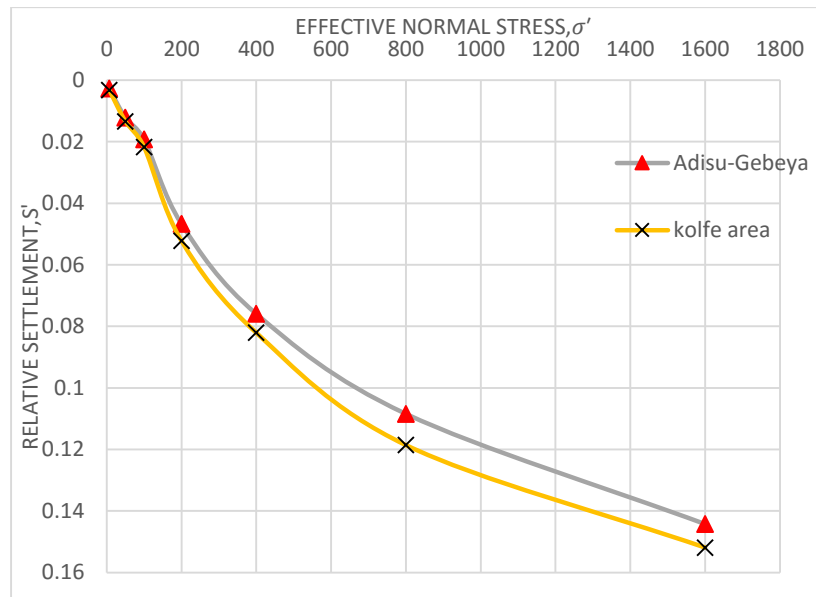


Fig. 3.5 Effective normal stress vs Relative settlement of Red clay samples on linear scale

3.6 Laboratory Results and Discussion

As it has been illustrated in Figure 3.2, the plot of vertical effective stress vs void ratio on a semi-log and linear scale show that except their variation in natural void ratio the plot show similar curvature for both the samples. The samples have a pre-consolidation pressure of 220 kPa and 260 kPa for Adisu-Gebeya and kolfe area respectively. Over-consolidation ratios of the soils are 2.86 and 5.6 for Adisu-Gebeya and kolfe area respectively, which is more than one. Hence the soils in this study area are over-consolidated in their natural state. Soils from these area are also over-consolidated in their natural state according to Samuel T.,1989 and Merihun L., 2010.

As shown in Figure 3.2 the value of compression index for red clay samples from Adisu-Gebeya and Kolfe area are 0.215 and 0.23 respectively. From the same figure values of re-compression index 0.055 and 0.059 are obtained for both Adisu-Gebeya and Kolfe area respectively.

Chapter 4: Constitutive model used for the numerical analysis

4.1 General

Numerical modelling continues to play a unique and intrinsic role in the process of geotechnical design. Of greatest concern are soil constitutive models that are employed with in finite element software to predict actual soil behaviour. There exist a large variety of models which have been recommended in recent years to represent the stress-strain and failure behaviour of soils. All these models inhibits certain advantages and limitations which largely depend on their application. Alternatively, Chen (1985) provided three basic criteria for model evaluation. The first criteria is theoretical evaluation of the models with respect to the basic principles of continuum mechanics to ascertain their consistency with the theoretical requirements of continuity, stability and uniqueness.

Secondly, experimental evaluation of the models with respect to their suitability to fit experimental data from a variety available test and the ease of the determination of the material parameters from standard test data. The final criteria is numerical and computational evaluation of the models with respect to the facility which they can be implemented in computer calculations.

In general, the criterion for the soil model evaluation should always be a balance between the requirements from the continuum mechanics aspect, the requirements of realistic representation of soil behaviour from the laboratory testing aspect (also the convenience of parameters derivation), and the simplicity in computational application.

4.2 Basics of the Modified Drucker-Prager/cap plasticity model

The Drucker–Prager/cap plasticity model has been widely used in finite element analysis programs for a variety of geotechnical engineering applications. This model is intended to simulate the constitutive response of cohesive geomaterials. A “cap” yield surface is added to the linear Drucker-Prager model. The two main purpose of the cap are to bind the model in hydrostatic compression as well as help to control the volumetric dilatancy. This model is appropriate to simulate soil behavior because it is capable of considering the effect of stress history, stress path, dilatancy and the effect of intermediate principal stress. The yield surface of this model consists of three parts: a Drucker-Prager shear failure surface, an elliptical cap, which

intersects the mean effective stress axis at a right angle, and a smooth transition region between the shear failure surface and the cap, as shown in the figure 4.1 (Abaqus tutorial 2002).

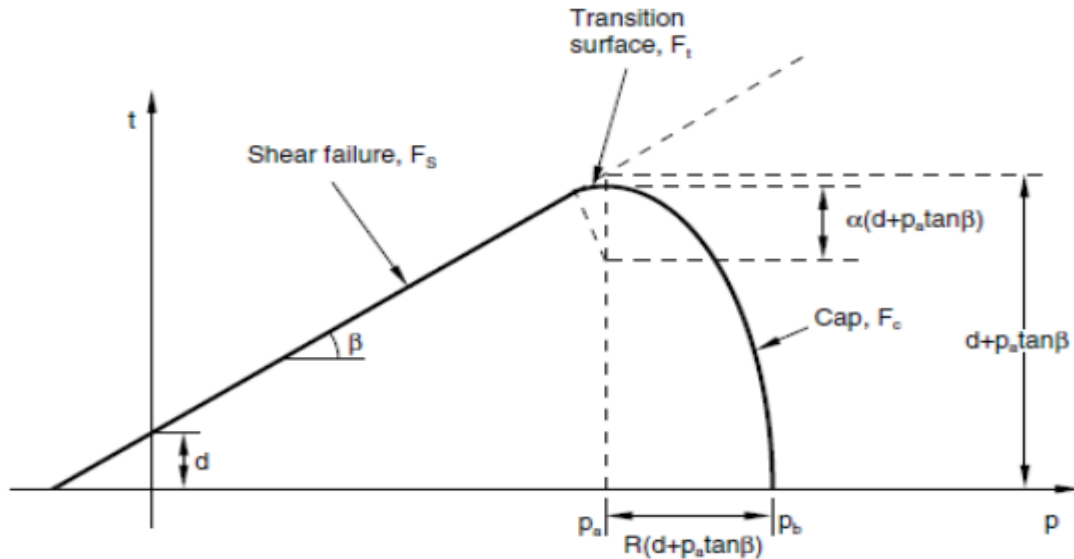


Fig.4.1 Modified Drucker-Prager/Cap model: yield surfaces in the p–t plane. (Adapted from Abaqus 2002).

The model uses associated flow in the cap region and non-associated flow in the shear failure and transition regions.

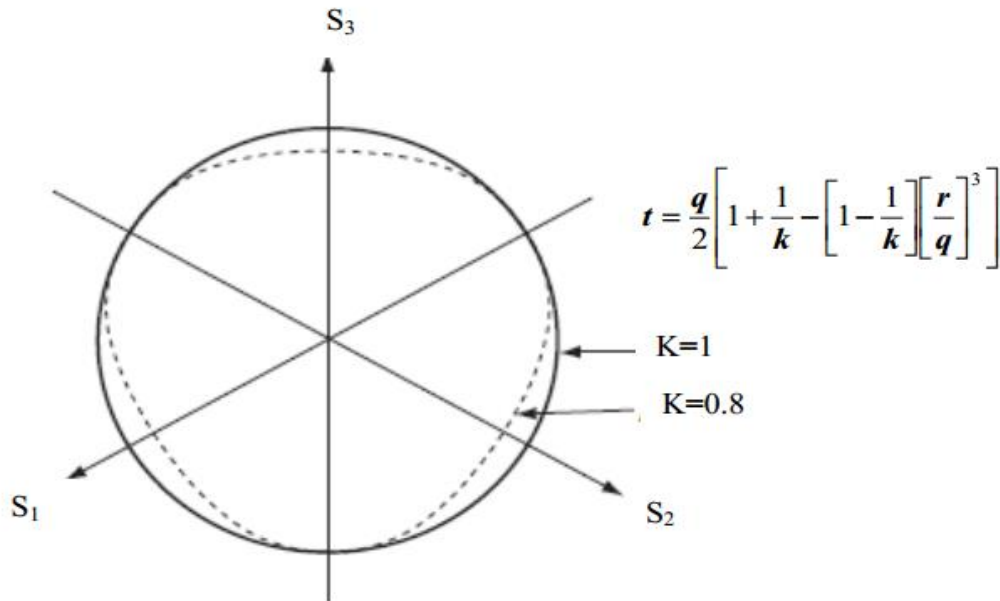


Fig. 4.2 Projection of the modified cap yield surface on the π -plane (Abaqus,2002).

The failure surface of this model is given by (S. Helwany,2007):

$$F_s = t - p \tan \beta - d = 0 \dots \dots \dots (4.1)$$

Where;

$$t = q/2 \left[1 + \frac{1}{k} - \left[1 - \frac{1}{k} \right] \left[\frac{r}{q} \right]^3 \right]$$

$$q = \sqrt{\frac{1}{2}((\sigma_1 - \sigma_2)^2 + (\sigma_2 - \sigma_3)^2 + (\sigma_3 - \sigma_1)^2)}$$

$$p = 1/3 (\sigma_1 + \sigma_2 + \sigma_3)$$

Where; q= deviatoric stress

P= hydrostatic stress

K= shape parameter of the yield surface Fs determined from triaxial compression and extension tests with usual values, 0.778<k<1.

d = Cohesion of the soil in the p-t plane

β = Slope of the yield surface Fs in the p-t plane

The cap yield surface is an ellipse with an eccentricity=R in the p-t plane as shown in the figure above. It is dependent on the third stress invariant, r in the deviatoric plane. The cap surface hardens (expands) or softens (shrinks) as a function of the volumetric plastic strain. When the stress state causes yielding on the cap, volumetric plastic strain (compaction) results, causing the cap to expand (hardening). But when the stress state causes yielding on the Drucker–Prager shear failure surface, volumetric plastic dilation results, causing the cap to shrink (softening). The cap yield surface is given by (S.Helwany, 2007):

$$F_c = \sqrt{(P - P_a)^2 + \left(\frac{Rt}{1+\alpha-\alpha/\cos\beta}\right)^2} - R(d + p_a \tan\beta) = 0 \dots \dots \dots (4.2)$$

Where R is a material parameter that controls the shape of the cap and α is a small number (typically, 0.01 to 0.05) used to define a smooth transition surface between the Drucker-Prager shear failure surface and the cap defined below.

$$F_t = \sqrt{(P - P_a)^2 + (t - (1 - \frac{\alpha}{\cos\beta})(d + p_a \tan\beta))^2} - \alpha(d + p_a \tan\beta) = 0 \dots \dots \dots (4.3)$$

where P_a = an evolution parameter that controls the hardening-softening behavior as a function of the volumetric plastic strain.

$$P_a = \frac{P_b - R d}{1 + R \tan\beta} \dots \dots \dots (4.4)$$

P_b is mean effective (yield) stress

The hardening–softening behavior is simply described by a piecewise linear function relating the mean effective (yield) stress P_b and the volumetric plastic.

$$\varepsilon_v^p = \frac{\lambda - k}{1 + e_o} \ln \frac{p'}{p'_o} = \frac{c_c - c_s}{2.3(1 + e_o)} \ln \frac{p'}{p'_o} \dots \dots \dots (4.5)$$

Where: ε_v^p = Plastic volumetric strain

c_c = Compression index

c_s = Swelling index

e_o = Initial void ratio

p'_o = Pre-consolidation pressure

p' = Effective (yield) stress

Equation 4.5 describes the evolution of plastic volumetric strain (the hardening parameter) with the mean effective stress. A graphic representation of the equation (cap hardening curve) is shown in Figure 4.3. The cap hardening curves of the samples are determined from Eq. 4.5 (S. Helwany, 2007).

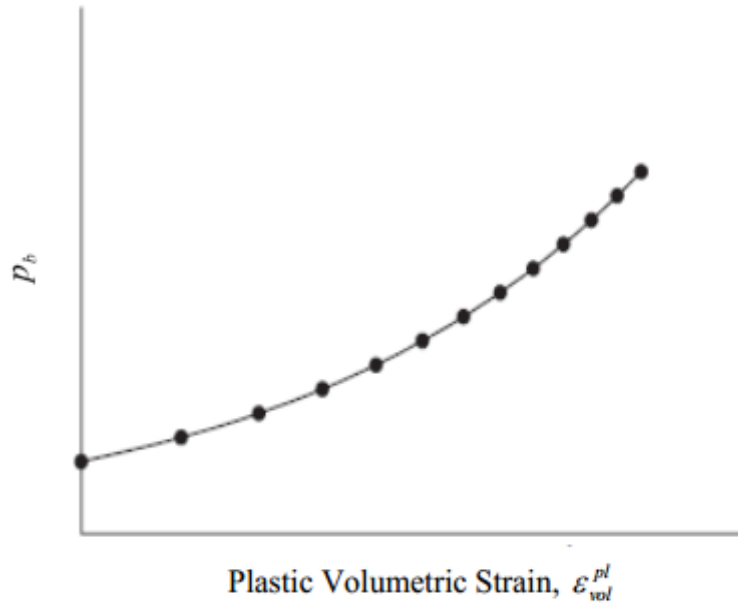


Fig. 4.3 Typical cap hardening behavior (Abaqus, 2002).

4.3 Cap hardening

The initial cap position is one of the input parameters for the cap model and can be obtained from the yield stress versus plastic volumetric strain plots with the value of P used as input parameter. The cap hardening behaviour of the red clay soils collected from different sites of Addis Ababa for each case are summarized in Table 4.1 to 4.3 based on Eq.4.5. The cap hardening curves of the red clay soils generated from eq.4.5 with their detailed calculation attached in Appendix C are shown in figures 4.4 to 4.6.

In this study a finite element software Abaqus was used to simulate the scenario. Basically, this finite element software mainly uses the concept of cap theory. Due to this, the Modified Drucker-Prager/Cap Plasticity model was used to simulate Oedometer test on red clay specimens.

Simulation of Oedometer test using Finite Element Method

Table 4.1 Cap hardening behaviour of Adisu Gebeya area red clay soils.

Adisu-Gebeya area red clay					
Case-1, using C_r		Case-2, using C_r & C_c		Case-3, using C_c	
ε_v^p	P_b	ε_v^p	P_b	ε_v^p	P_b
0	220	0	220	0	220
0.0225	397.63	0.0225	475.21	0.0225	532.65
0.0415	650.62	0.0415	688.36	0.0415	987.6
0.0525	926.71	0.0525	919.91	0.0525	1448.3
0.0635	1230.61	0.0635	1235.01	0.0635	2279.87
0.0775	1845.15	0.0775	1896.32	0.0775	4123.41
0.0925	2796.2	0.0925	3356.37	0.0925	6764.92
0.115	4668.7	0.115	6315.87	0.115	11587.02
0.135	7008.38	0.135	10531.96	0.135	16781.05
0.155	10239.57	0.155	16387.05	0.155	23512.43

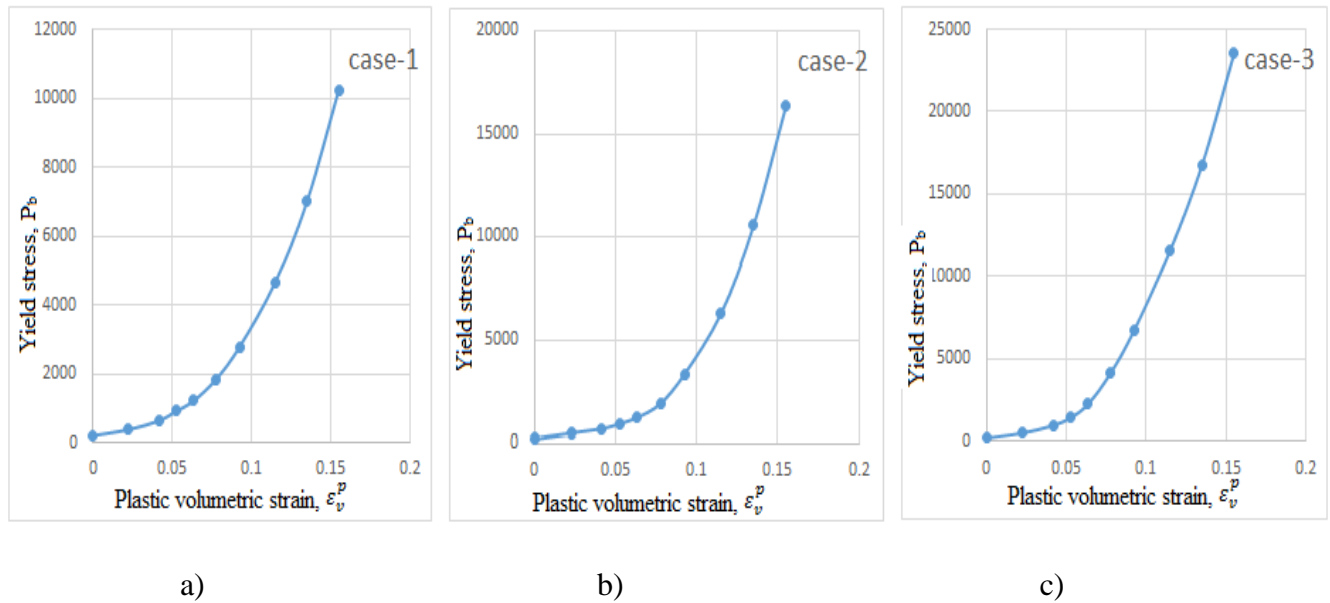


Fig. 4.4 Cap hardening curve for Adisu-Gebeya red clay; a) case-1 b)case-2 c) case-3

Table 4.2 Cap hardening behaviour of Kolfe area red clay soils.

Kolfe area red clay					
Case-1, using C_r		Case-2, using C_r & C_c		Case-3, using C_c	
ε_v^p	P_b	ε_v^p	P_b	ε_v^p	P_b
0	260	0	260	0	260
0.0225	359.34	0.0225	587.62	0.0225	687.62
0.0415	589.36	0.0415	985.31	0.0415	1385.31
0.0525	784.86	0.0525	1552.74	0.0525	1852.74
0.0635	1045.2	0.0635	2178.21	0.0635	2978.21
0.0775	1504.99	0.0775	4041.37	0.0775	4741.37
0.0925	2224.24	0.0925	6625.12	0.0925	7625.12
0.115	3996.24	0.115	11789.65	0.115	13789.65
0.135	6727.4	0.135	18521.37	0.135	20521.37
0.155	11325.09	0.155	26682.43	0.155	28682.43

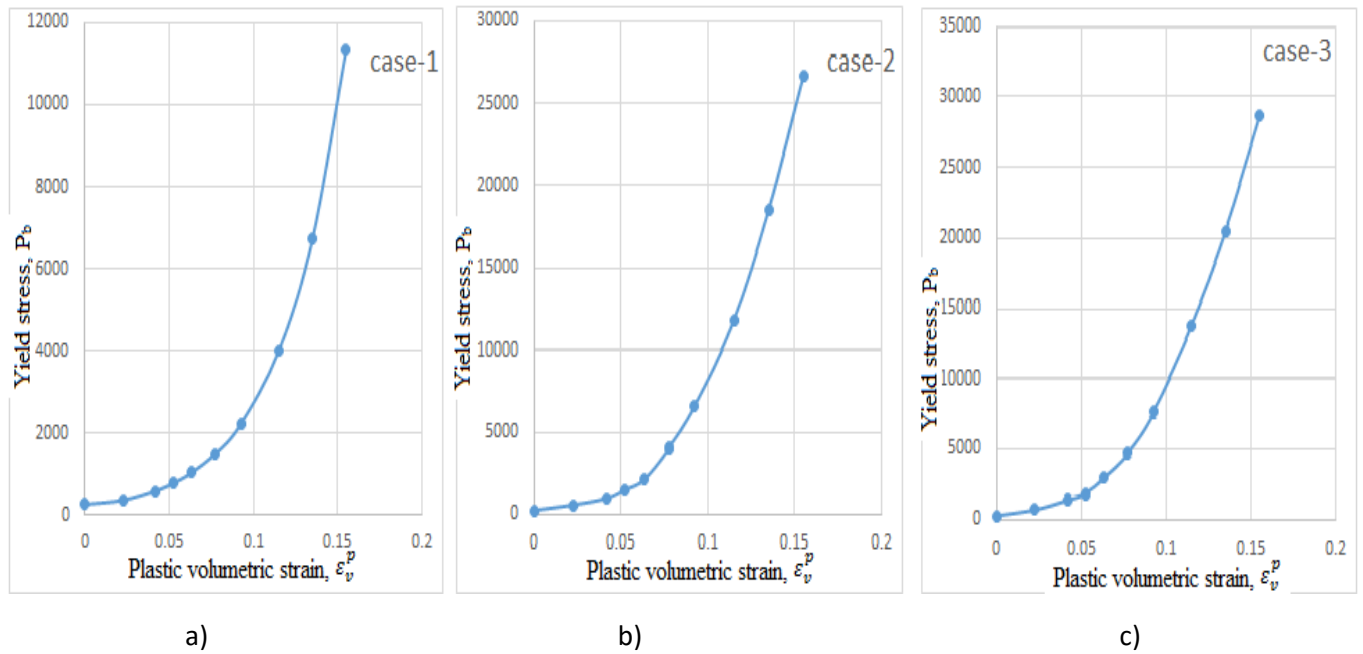


Fig. 4.5 Cap hardening curve for Kolfe area red clay; a) case-1 b) case-2 c) case-3

Table 4.3 Cap hardening behaviour of Rufael area red clay soils.

Rufael area red clay					
Case-1, using C_r		Case-2, using C_r & C_c		Case-3, using C_c	
ε_v^p	P_b	ε_v^p	P_b	ε_v^p	P_b
0	295	0	295	0	295
0.0225	412.35	0.0225	495.21	0.0225	542.65
0.0415	670.62	0.0415	698.36	0.0415	1087.6
0.0525	956.71	0.0525	979.91	0.0525	1548.3
0.0635	1330.61	0.0635	1335.01	0.0635	2379.87
0.0775	1945.15	0.0775	1996.32	0.0775	4223.41
0.0925	2896.2	0.0925	3456.37	0.0925	6864.92
0.115	4768.7	0.115	6415.87	0.115	12587.02
0.135	7108.38	0.135	11531.96	0.135	17781.05
0.155	11239.57	0.155	17387.05	0.155	24512.43

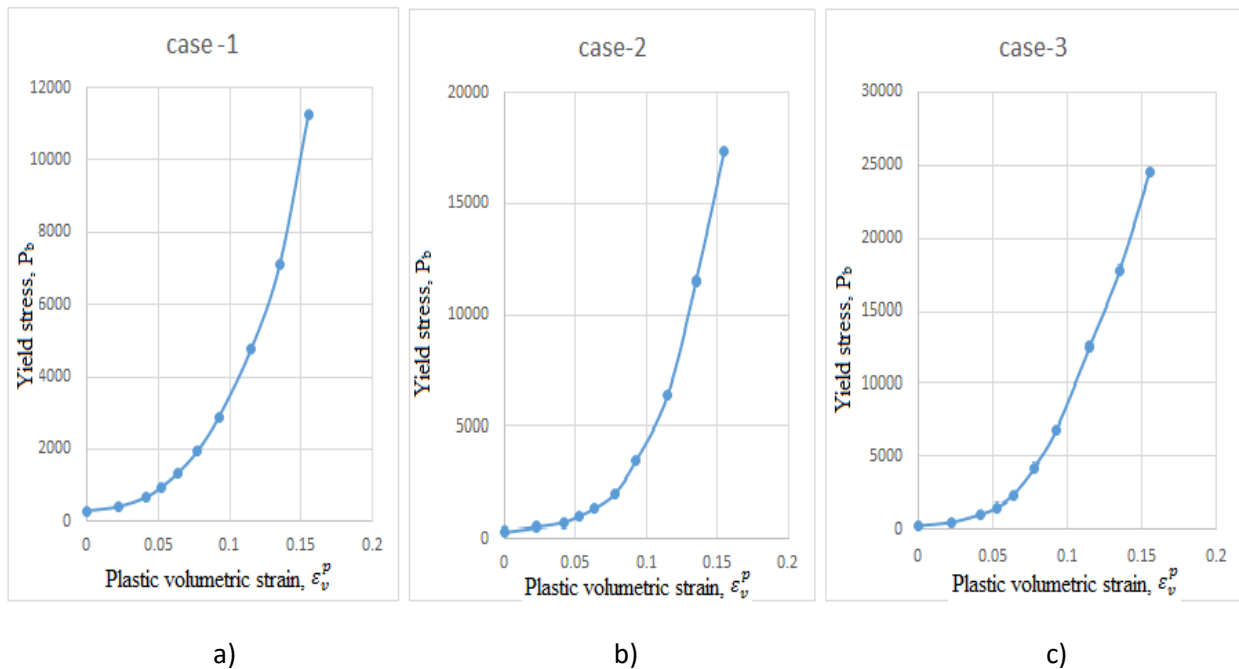


Fig. 4.6 Cap hardening curve for Rufael area red clay; a) case-1 b) case-2 c) case-3

4.4 Flow Rule

In this model the flow potential surface in the p-t plane consists of two parts as shown in figure 4.7. In the cap region the plastic flow is defined by a flow potential that is identical to the yield surface (i.e., associated flow). For the Drucker-Prager failure surface and the transition yield surface, a non-associated flow is assumed. In the cap region the elliptical flow potential surface is given as:

$$G_c = \sqrt{(P - P_a)^2 + \left(\frac{Rt}{1 + \alpha - \alpha/\cos\beta}\right)^2} \dots\dots\dots(4.6)$$

The elliptical flow potential surface portion in the Drucker-Prager failure and transition regions is give as

$$G_s = \sqrt{[(P_a - P)\tan\beta]^2 + \left(\frac{t}{1 + \alpha - \alpha/\cos\beta}\right)^2} \dots\dots\dots(4.7)$$

As shown in figure 4.7, the two elliptical portions, G_c and G_s , provide a continuous potential surface.

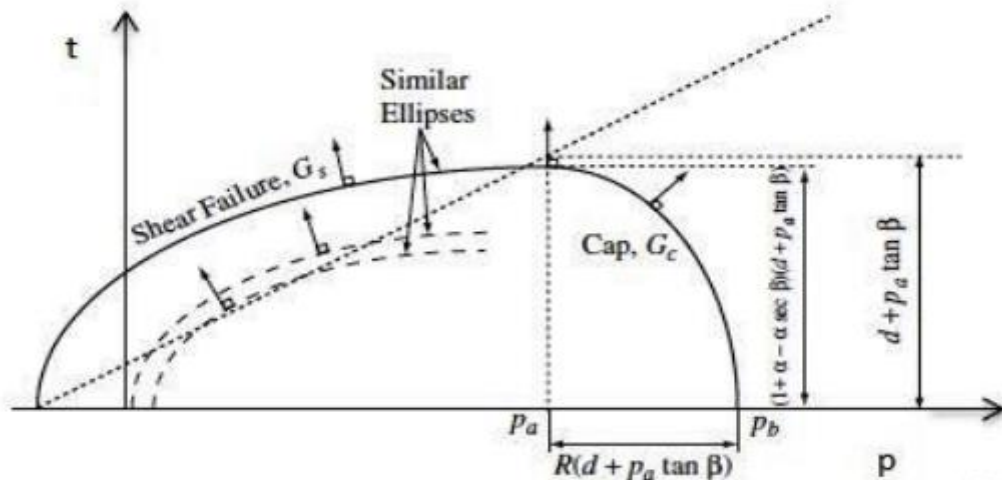


Fig. 4.7 Flow potential of the modified cap model in the p-t plane (adopted from Abaqus manual, 2002).

The Mohr-Coulomb model parameters (C, Ø) can be converted to Drucker-Prager parameters as follows:

$$\tan\beta = \frac{6\sin\phi'}{3 - \sin\phi'} \dots\dots\dots(4.8)$$

$$d = \frac{18C' \cos \phi'}{3 - \sin \phi'} \dots\dots\dots(4.9)$$

$$K = \frac{3 - \sin \phi'}{3 + \sin \phi'} \dots\dots\dots(4.10)$$

Where $0.778 < K < 1$

Basic soil parameters that are used as input in the Cap plasticity constitutive model are summerized as shown in Table 4.4. The elastic (E & ν), plastic (ϕ' & C') and γ parameters of the red clay specimens were collected from (Mustefa T., 2016, Samuel T., 1989, Merihun L., 2010, Soressa M., 2016, Yodit M., 2012 and Hailemariam A., 2005). Where as, corresponding β & d were computed from Eq. 4.8 & 4.9 respectively. The values of ϵ_{vol}^{pl} , R , α & K were also taken from the basic theories of Cap Plasticity model.

Table 4.4 Average basic soil parameters for the Red clay soils for Adisu Gebeya , Rufael and Kolfe area.

Soil parameter	Symbol	Unit	Addisu- Gebeya	Kolfe area	Rufael area
Modulus of elasticity	E	[MN/m ²]	11.14	10.67	10.21
Poisson's ratio	ν	[-]	0.3	0.3	0.3
Unit weight	γ	[kN/m ³]	19.13	18.61	18.05
Angle of internal friction	ϕ'	[°]	26.5	25	26
Cohesion	C'	[kN/m ²]	23	26.58	23.5
Slope of the yield surface Fs in the p-t plane	β	[°]	46	44.5	48.1
Intersection of yield surface Fs with the t-axis	d	[kN/m ²]	125.2	153.8	122.4
Initial cap position	ϵ_{vol}^{pl}	[-]	0	0	0
Cap eccentricity	R	[-]	0.8	0.8	0.8
Transition surface radius	α	[-]	0.03	0.03	0.03
Flow stress ratio	K	[-]	0.788	0.788	0.788

Chapter 5: The Finite Element Method (FEM) results and discussion

5.1 General

The finite element method is a common tool within various fields of engineering. It is used for advanced numerical calculations and is developed from the theories of continuum mechanics, which studies equilibrium, motion and deformation of physical solids. FEM prerequisites that the mathematical models which describe the motions of the media has to be based on continuous functions. In FEM the continuous functions are approximated by a discrete model where the body to be studied is divided into several smaller parts, so-called elements. The discretized model is composed by a number of element functions that are continuous over each separate element. These elements are connected in nodes, which is primarily where the calculations are made. Numerical values for the nodes are compiled to make the element functions an accurate approximation of the global function. Accuracy improves when the number of nodes increases. The element functions are gathered in the global equation system containing material and geometrical data. The forces applied on the element geometry are represented by load vectors that act in the nodes. The matrixes quickly increase in size and demand high computer performance to be solved. The nodal deflections are the solution to the equation system. The values between the nodes are received by interpolation with either linearly approximations or polynomials of n degrees (Gabrielsson, 2007).

Generally analysis using Abaqus involves two major procedures, viz, preprocessing and postprocessing.

5.2 Preprocessing

It comprises all the steps to create the model with Abaqus/CAE. The following principal steps are taken sequentially:

I - Creating a part /defining the model geometry

The first step in creating the model is to define its geometry. The model is created with a two-dimensional, deformable body with a solid, extruded base feature. An axis-symmetric geometrical model with 25 mm in x-axis direction and 20 mm in y-axis direction is set to

simulate a standard IL test sample (20 mm in height and 50 mm in diameter) as shown in Figure 5.1.

II-Defining the material and section properties

The next step in creating the model involves defining and assigning material and section properties to the part. Each region of a deformable body must refer to a section property, which includes the material definition. In this model linear elastic materials are created for the red clay specimens.

III-Creating an assembly

The geometry of the assembly is defined by creating instances of a part and then positioning the instances relative to each other in a global coordinate system.

IV- Configuring the analysis

Analysis steps can be broadly categorized as an initial step and analysis steps. They are dealt subsequently.

a) The initial step

Abaqus/CAE creates a special initial step at the beginning of the model's step sequence and names it Initial. It allows defining boundary conditions and predefined fields such as void ratio of the sample. The actual in situ stress initial condition of the soil mass is simulated in this step and equilibrium condition of the internal stress is checked here.

b) Analysis steps

The initial step is followed by one or more analysis steps. Each analysis step is associated with a specific procedure that defines the type of analysis to be performed during the step.

V-Applying boundary conditions and applied loads

Prescribed conditions, such as loads and boundary conditions, are step dependent, which means that the step or steps in which they become active is specified accordingly.

a) Boundary condition

The boundary conditions of the finite element mesh shown in Figure 5.1 are as follows. On the bottom side, both the vertical and horizontal components of the displacement are fixed ($U_x=U_y=0$), and on the right-hand side, the horizontal component of displacement is fixed ($U_x=0$) to simulate the frictionless interface between the soil and the ring. The left-hand side of the mesh is a symmetry line (no horizontal displacement). Note that, the ring is not modeled in the analysis and flow of pore water through the walls of the ring is not allowed.

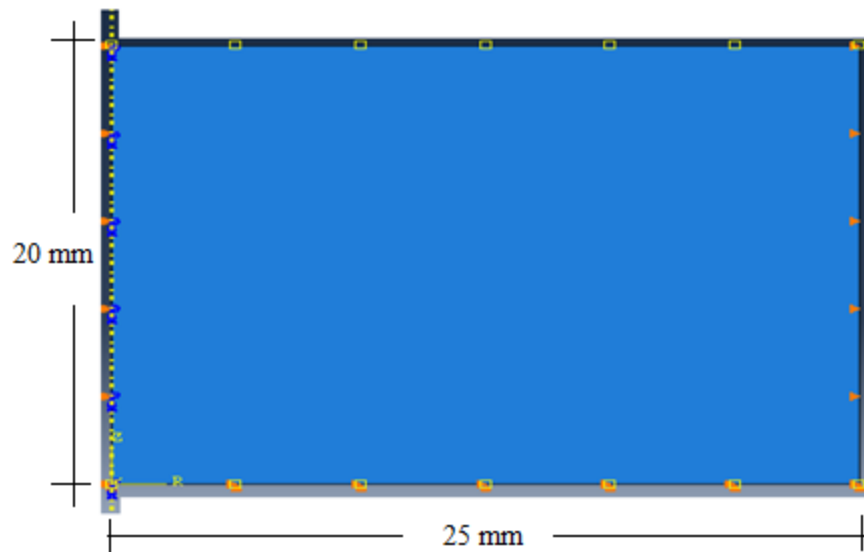


Fig. 5.1 Symmetrical part and boundary condition of the sample.

b) Applying load

In this step, the test loads are applied in an incremental manner to simulate the actual oedometer test procedures. There are two types of load application methods in numerical models. The first is by applying direct loads on the top of the sample and the second one is by applying a predetermined displacement on the top of the sample. But in this study the first load application method which is applying direct loads on the top of the sample is used.

VI- Designing the mesh

The Mesh module contains tools that allow generating meshes on parts and assemblies created within Abaqus/CAE. The element chosen is a pore fluid/stress four-node axisymmetric quadrilateral element with bilinear displacement and bilinear pore pressure. At the beginning of the simulation coarser meshing was used and the results obtained are inconsistent with the

laboratory test results. Finally, by changing element size fine mesh was used hence the results obtained from the finite element analysis become close to the laboratory results. The selected mesh size is 0.0065 as shown in Figure 5.2.

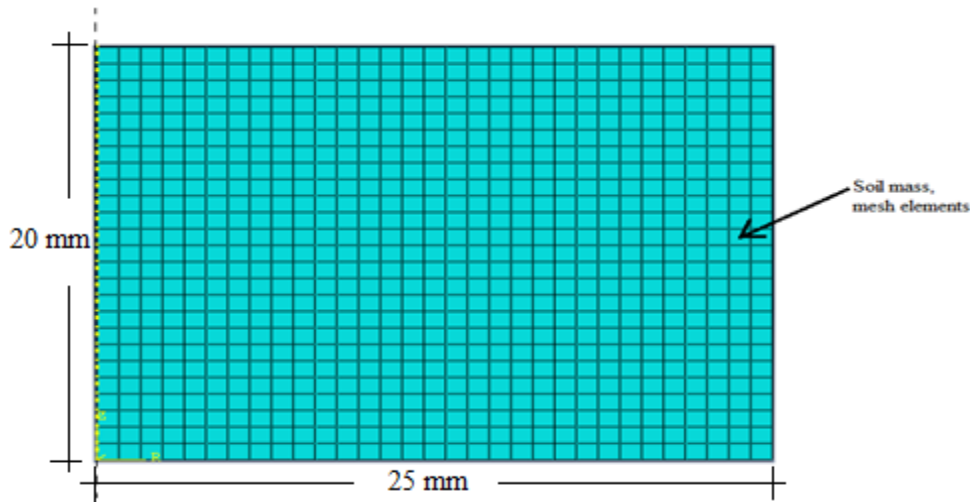


Fig. 5.2 Discretised model

VII- Creating, running, and monitoring a job

Once defining a model is finished, the model is analyzed using the Job module. The Job module allows interactively submitting a job for analysis and monitoring its progress.

5.3 Postprocessing

The Visualization module provides graphical display of finite element models and results. It obtains model and result information from the output database; it is controlled what information is written to the output database by modifying output requests in the Step module.

5.4 Simulation of drained condition

Since one-dimensional consolidation test in clay soils is time dependent process which needs enough time for excess pore water to drain out from the clay sample. The drained (long term) condition will best simulate the model with the actual oedometer test. Four main measures must be considered for a successful finite element analysis of soils considering their long-term (drained) behavior (Sam Helwamey, 2007).

(I) The initial conditions of the soil strata (initial geostatic stresses, initial pore water pressures, and initial void ratios) must be estimated carefully and implemented in the analysis. The initial conditions will determine the initial stiffness and strength of the soil strata;

(II) The boundary conditions must be defined carefully as being pervious or impervious;

(III) The long-term strength parameters of the soil must be used in an appropriate soil model; and

(IV) loads must be applied slowly. Slow loading does allow enough time for the pore water pressure to dissipate, thus invoking the long-term strength of the soil. This means that there is no need to input the long-term strength parameters because the constitutive model will react to slow loading in an “drained” manner.

5.5 Finite element results

In this thesis, a finite element software abaqus was used to simulate the Oedometer tests performed on red clay specimens. The finite element models was modelled having the same dimension as the samples used in the one-dimensional consolidation test in laboratory. Once, modelling of a single clay sample is carried out the remaining samples were modelled using the first as a templet. The applied stress on the one-dimensional cell were presented as a uniform distributed load and applied incrementally on the models. Boundary condition for pore water pressure was also provided during application of the loads. During simulation of the Oedometer test three different cases were considered.

Case-1: When the effective overburden pressure and the increase in pressure due to the applied loads not exceed the determined value of pre-consolidation pressure.

In this case, only the re-compression index, C_r is considered during simulation of the compression phenomenon and this C_r value can be determined from the curve between effective overburden pressure up to the pre-consolidation pressure of the void ratio versus log pressure curve of the samples.

Case-2: When the effective overburden pressure is less than pre-consolidation pressure and the increase in pressure due to the applied loads exceed the determined value of pre-consolidation pressure.

Simulation of Oedometer test using Finite Element Method

In this case, both re-compression, and compression indices are considered during simulation of the scenario. The value of re-compression index can be computed as it is stated in case-1 and the compression index, C_c value can be determined from the straight portion of the loading curve in e - $\log p$ curve.

Case-3: When both the effective overburden pressure and the increase in pressure due to the applied loads exceed the determined value of pre-consolidation pressure. In this case, only the compression index, C_c is considered during simulation of Oedometer test. The value of compression index can be computed as it is stated in case-2.

Simulation of Oedometer test for the red clay samples collected from the selected area of Addis Ababa were carried out (Table 4.4) and the finite element analysis results obtained from the software are shown in appendix D.

Typical finite element analysis results of settlement values expressed in units of meter are shown below in Fig. 5.3 to Fig. 5.5 for Adisu Gebeya, Kolfe and Rufael area red clay soil.

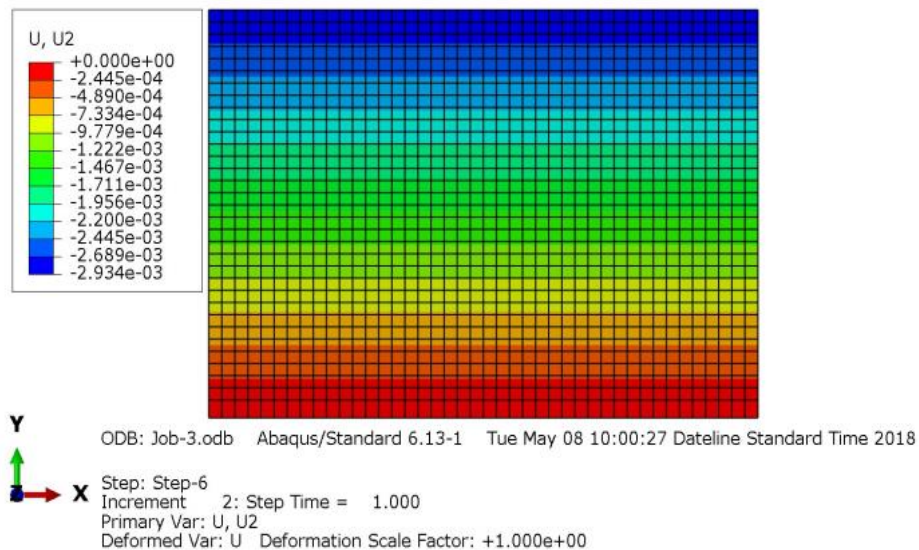


Fig. 5.3 FEM result for Adisu Gebeya red clay, case-1.

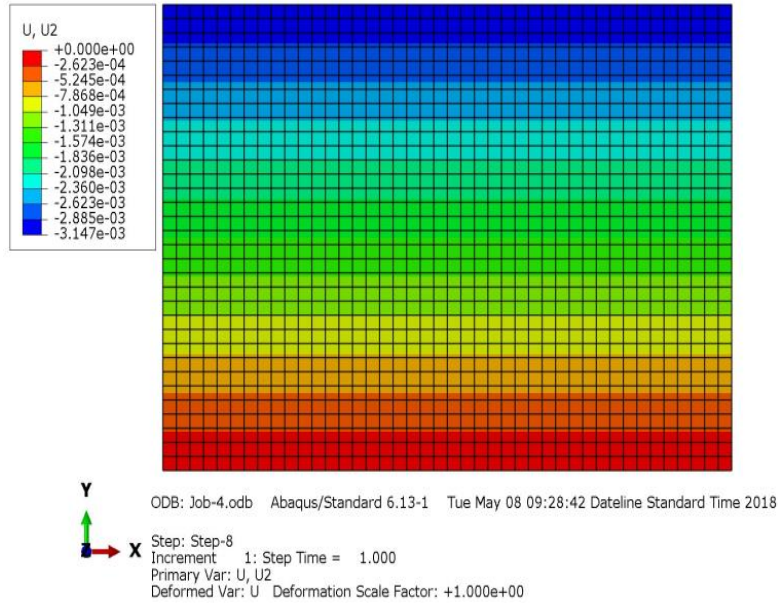


Fig. 5.4 FEM result for Kolfe area red clay, case-1

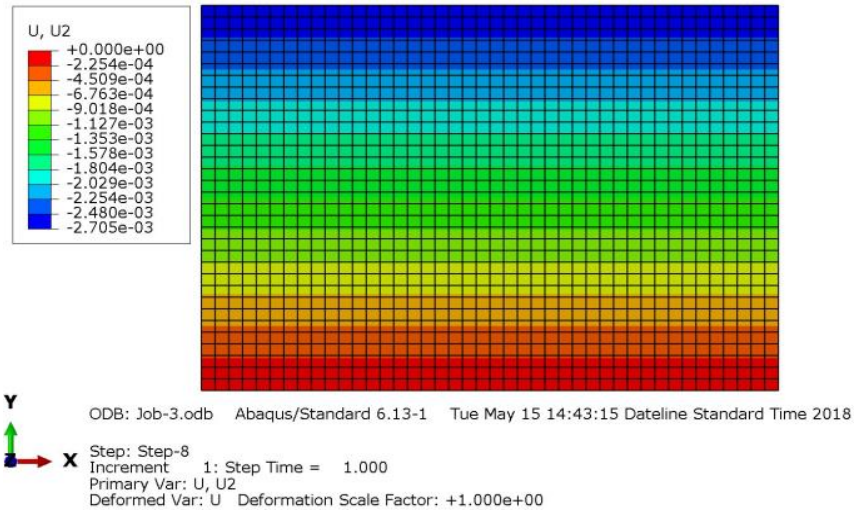


Fig. 5.5 FEM result for Rufael area red clay, case-1

Effective normal stress versus relative settlement graphs were generated from the finite element analysis using Cap Plasticity model for all the three different cases and these numerical analysis results are compared with the respective actual Oedometer test results as shown in Fig. 5.6 to Fig. 5.8.

Simulation of Oedometer test using Finite Element Method

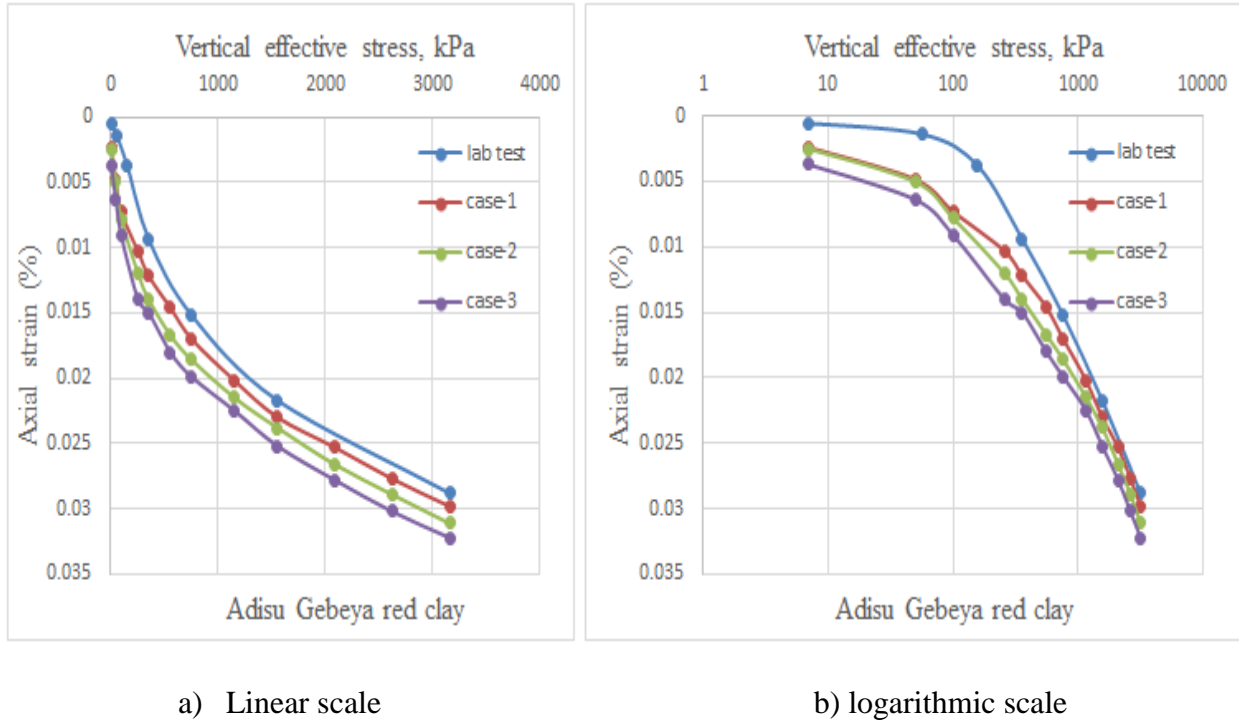


Fig. 5.6 Comparison of FEM result with the Oedometer test for Adisu-Gebeya red clay sample.

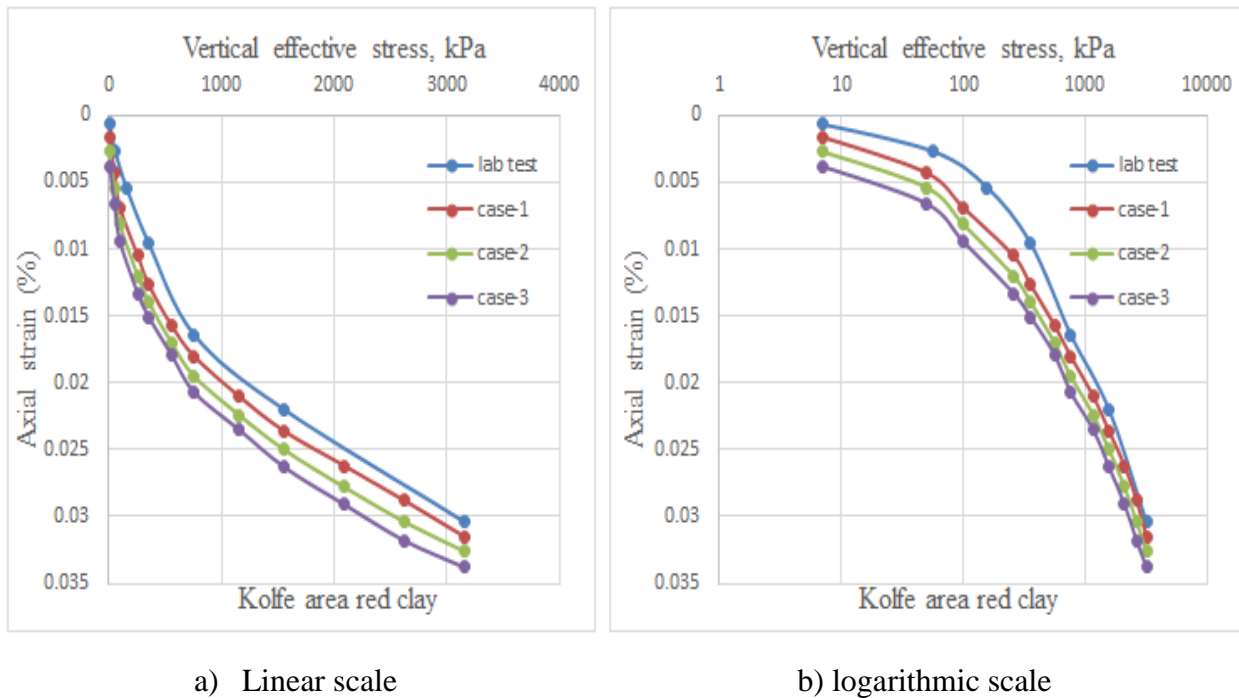


Fig. 5.7 Comparison of FEM result with the Oedometer test for Kolfe area red clay sample.

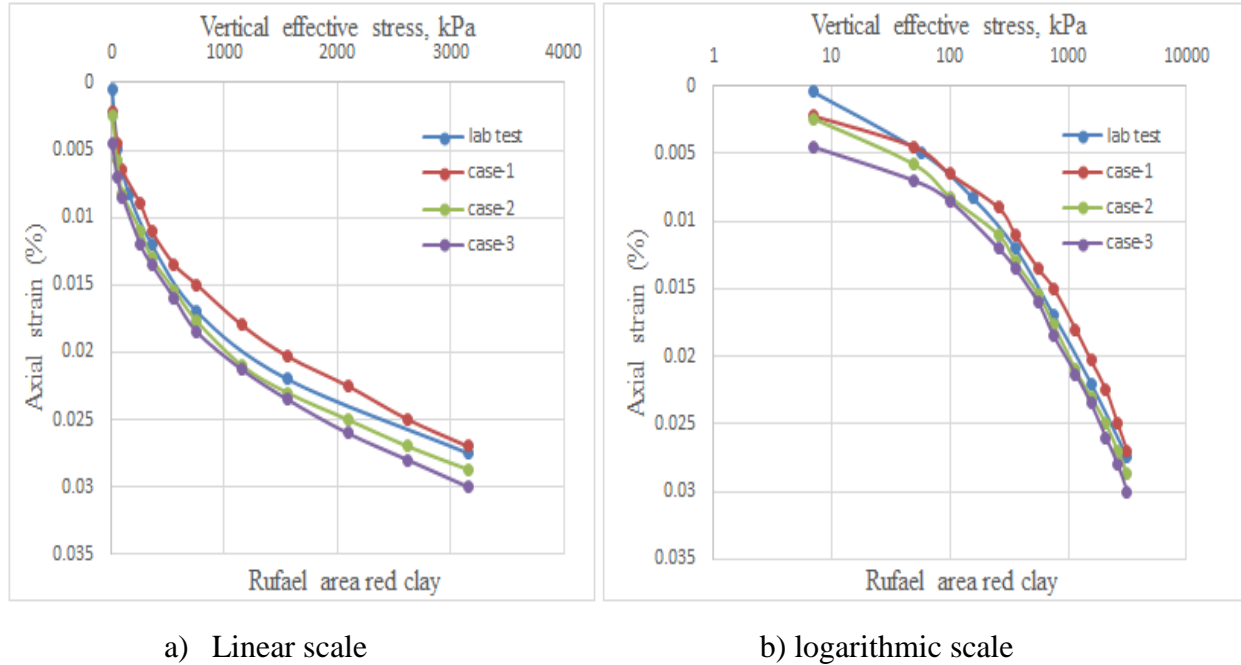


Fig. 5.8 Comparison of FEM result with the Oedometer test for Rufael area red clay sample.

As it has been illustrated in Figures 5.6, 5.7 and 5.8, the generated compressibility curves for each of the three different cases from the finite element analysis and the compressibility curves obtained from the one-dimensional consolidation tests for the Redclay specimens collected from Adisu-Gebeya, Kolfe and Rufael area respectively shows similar nature of deformation. The relative settlements at the end of compression from the finite element analysis are also close to the results obtained from the one-dimensional consolidation tests.

Comparison of finite element analysis results with one-dimensional consolidation test was made and presented in a tabular form as shown in Table 5.1.

Table: 5.1 Comparison of relative settlement from laboratory and FEM results.

Location	Laboratory Results (mm)	FEM results using Cap Plas. (mm)			Difference (%)		
		Case-1	Case-2	Case-3	Case-1	Case-2	Case-3
Adisu-Gebeya	0.144	0.149	0.156	0.161	0.5	1.2	1.7
Kolfe area	0.152	0.157	0.163	0.169	0.55	1.1	1.7
Rufael area	0.137	0.135	0.144	0.150	0.18	0.65	1.3

As it is shown in Table 5.1, the maximum difference value obtained from the finite element analysis and one-dimensional consolidation test for the first case on the sites under consideration is 0.55% from Kolfe area specimen. From the same Table, the maximum difference value obtained from the finite element analysis and one-dimensional consolidation test for the second case on the sites under consideration is 1.2% from Adisu-Gebeya area specimen. Similarly, the maximum difference value obtained from the finite element analysis and one-dimensional consolidation test for the third case on the sites under consideration is 1.7% from both Adisu-Gebeya and Kolfe area specimens.

R.J. Filipe, 2001 and Asad H., 2016 carried out simulation of Oedometer test on cohesive and cohesionless materials using different constitutive models. R.J. Filipe, 2001 was used Cap Plasticity model to simulate the phenomenon on clay soils using a finite element software Plaxis 2D. Similarly, Asad H., 2016 was used Hardening soil model to simulate the scenario on both dense and loose sand using a finite element software Plaxis 2D.

The relative settlement results obtained at the end of compression as shown in Figures 2.9 and 2.10, the finite element analysis results for both the studies are very close to the results obtained from the laboratory one. Both Filipe, 2001 and Asad, 2016 recommended to use these compressibility curves to determine the strain corresponding to the additional pressure exerted due to the proposed structure. Hence, these results have been used to determine a strain for the corresponding additional pressure exerted due to the applied loads for the specific sites under consideration. Similarly, the finite element results obtained from this Thesis are very close to the laboratory results as it is shown in Table 5.1 for all the three different cases and hence can be used to determine the strain corresponding to the additional pressure exerted due to the applied loads for the specific sites under consideration.

Chapter 6: Conclusion and Recommendation

6.1 Conclusion

Numerical analysis method, such as finite element method, is widely used to predict the bearing capacity and settlement of foundations. ABAQUS, as a general-purpose finite element analysis software package, is commonly used in geotechnical engineering, due to its powerful capability in non-linear analysis. In this Thesis, simulation of oedometer test using FEM analysis was examined and the resulting effective normal stress versus relative settlement curves are compared with actual Oedometer test results. Based on the results obtained from both the actual one-dimensional consolidation tests and simulation by Abaqus, the following conclusions can be drawn.

- The finite element analysis results obtained using Cap plasticity (modified Drucker-Prager) model gives close simulation results when compared with the actual oedometer test results. This is due to the cap and the associated hardening considered in the cap model.
- The generated compressibility curves obtained from the finite element analysis results using the Cap Plasticity model shows similar nature of deformation in all the three cases when compared with the compressibility curves obtained from the laboratory test for the specific sites considered in this study.
- Due to the closeness of the results obtained from the finite element analysis and the one-dimensional consolidation test, these generated compressibility curves can be used to determine the corresponding strain for the additional pressure exerted by the applied surcharge loads on the specific area considered in this study.
- Incorporating actual soil data and parameters that can best describe the soil formation under consideration, and by selecting a proper constitutive soil models and theories, simulation results of Oedometer test can be taken as one alternative to estimate strain corresponding to the additional pressure due to the applied loads for red clay soils from selected area of Addis Ababa.

6.2 Recommendation

- Samples were collected from Adisu-Gebeya and Kolfe area where red clay soils are mainly found based on geological drilling data and Addis Ababa map. But, for better simulation of Oedometer test samples should be collected from various area where red clay soils are dominantly found.
- In this Thesis, only Cap plasticity model was used during the finite element analysis among the various constitutive soil models to simulate the Oedometer test using a finite element software called ABAQUS. Further studies should be conducted using other constitutive material models relevant to the specific soil under consideration.
- Despite the fact that, some of the soil parameters required for numerical analysis used in this Thesis are obtained directly from laboratory test results, some soil parameters are also used from secondary data. A better simulation result of FEM could have been obtained, if all soil parameters have been directly determined from laboratory test results.
- In this study only the loading procedures of the test are considered during simulation of the Oedometer test. To get all the settlement parameters and better simulation of the test, further studies should be conducted considering the unloadings of the loading-reloading procedures.

Reference

1. Abaqus Inc., (2013). "Pawtucket, RI. Abacus User's manual-version 6.13-1".
2. R. Ziaie Moayed, S. Tamassoki, and E. Izadi,(2012). "Numerical modelling of direct shear tests on sandy clay". International journal of Civil, Environmental, Structural, Construction and Architectural Engineering Vol: 6, No: 1.
3. Mohammed Y. Fattah, Firas A. Salman and Bestun J. Nareeman,(2011). "Numerical simulation of triaxial test in clayey soil using different constitutive relations". Advanced Materials Research, vols. 243-249, pp. 2973-2977.
4. S. Helwany,(2007). "Applied soil mechanics with Abaqus application",John Wiley & Sons, Inc., Hoboken, New Jersey.
5. Plaxis version 8 material models manual.
6. Mats Kahlstrom,(2013). "Plaxis 2D comparison of Mohr-Coulomb and Soft soil material models". M.Sc. Thesis Presented to School of Graduate Studies, Lulea university of Technology, Sweden.
7. P. Gustafsson,(2011). " Numerical study of different creep models used for soft soils". M.Sc. Thesis Presented to School of Graduate Studies, Chalmers university of Technology, Sweden.
8. Belay Z.,(2015). " Simulation of pile load test using finite element method".M.Sc. Thesis Presented to School of Graduate Studies, Addis Ababa Institute of Technology, Addis Ababa.
9. Fitsum T.,(2011). " Analysis of deformations in soft clay due to unloading". M.Sc. Thesis Presented to School of Graduate Studies, Chalmers university of Technology, Sweden.
10. Samuel T.,(1989). "Investigation into some of the engineering properties of Addis Ababa red clay soils". M.Sc. Thesis Presented to School of Graduate Studies, Addis Ababa University, Addis Ababa.
11. Hailemariam A.,(2005). "Investigation into shear strength characteristics of red clay soil of Addis Ababa". M.Sc. Thesis Presented to School of Graduate Studies, Addis Ababa University, Addis Ababa.
12. Bishop, A.W./Henkel,D.J.,(1962). "The measurement of soil properties in the triaxial test", London.

13. ASTM,(2004).“Special Procedures for Testing Soil and Rock for Civil Engineering Purpose”, U.S. America.
14. Arora, K.R.,(2004).“Soil Mechanics and Foundation Engineering”, Standard Publishers & Distributors, New Delhi.
15. Kok Sien Ti,(2009). “A review of basic soil constitutive models for geotechnical applications”. EJGE.
16. Dipika Devi,(2013).“On the determination of modified cam clay model parameters”. National Conference on Recent Advances in Civil Engineering (NCRACE).
17. M. Murat Monkul & Okan Onal,(2004).“A visual basic program for analyzing oedometer test results and evaluating inter granular void ratio”. Computers and Geosciences.
18. Sushed Likitlersuang,(2003). “A Hyper plasticity model for clay behavior: An application to Bangkok clay”. Ph.D. dissertation, University of Oxford.
19. Potts, D.M. and Zdravkovic, L.,(1990, 2001). “ Finite Element Analysis in Geotechnical Engineering”, Vol.1: theory, Vol.2 Application, Thomas Telford Publishing.
20. Budhu, M.,(2000). “Soil Mechanics and Foundations”, John Wiley and Sons, U.S America.
21. Murthy, V. N. S.,(1990).“Geotechnical Engineering: Principles and Practices of Soil Mechanics and Foundation Engineering”, Marcel Dekker, Inc., New York.
22. Asad H.,(2016). “ Prediction of one-dimensional compression test using finite element method”. International Journal of Engineering Research & Technology, University of Wasit, Wasit, Iraq.
23. P. Lenk,(2009). “ Modelling of Primary Consolidation”. Slovak Journal of Civil Engineering, Slovak University of Technology, Radlinskeho 11, Bratislava.
24. R.J.Filipe,(2001). “ Oedometer test contribution for the study of deformation in oil reservoirs”. International Journal of Civil Engineering, Instituto Superior Tecnico, Avenida Rovisco Pais.
25. Yuan, Yixing, and Andrew J. Whittle,(2013). “ Examination on Time- Dependent soil Models in One-Dimensional Consolidation Test”. Springer Series in Geomechanics and Geoengineering, MIT.

26. Jibril J.,(2011). “Correlation between critical state soil parameters and index properties of undisturbed red clay soils in Addis Ababa”. A thesis presented to School of Graduate Studies, Addis Ababa University, Addis Ababa.
27. Merihun L.,(2010). “A Study on the Effect of Remolding on the Mechanical Behavior of Addis Ababa Red Clay Soils”. M.Sc. Thesis Presented to School of Graduate Studies, Addis Ababa University, Addis Ababa.
28. Alemayehu T. and Mesfin L.,(1999). “Soil Mechanics” Faculty of Technology, Addis Ababa University, Addis Ababa.
29. Kebede T. and Tadesse H., (1990). “Engineering Geological Mapping of Addis Ababa”, Ethiopian Geological Survey, Addis Ababa, Ethiopia.
30. Lamesgin M., (2014). “Bearing Capacity Assessment for Building Foundations Using Different Approaches- A Comparative Study at Addis Ababa, Central Ethiopia”. MSc. Thesis, Addis Ababa University Department of Earth Science, Engineering Geology, Addis Ababa.
31. Morin, W.J., and Parry, W.T.,(1971). “Geotechnical Properties of Ethiopian Volcanic Soils”, *Geotechnique* Vol. 21, No 3, 223-232.
32. Hansbo S., (1975). *Soil material science*. AWE/GEBERS, Stockholm, Sweden.
33. Larsson R., (1986). “Consolidation of soft soils”. Swedish Geotechnical Institute Report 29, Linköping, Sweden.
34. Sällfors G., (1975). “Preconsolidation pressure of soft, high plastic clays”. Ph.D. thesis, Geotechnical Department, Chalmers University of Technology, Gothenburg, Sweden.
35. Vermeer P.A. & Neher H.P., (1999). “A soft soil model that accounts for creep”. *Proceedings of the Plaxis Symposium on Beyond 2000 in Computational Geotechnics*, Amsterdam, the Netherlands.
36. Das, B. M. (2008). *Advanced Soil Mechanics* (3rd ed.). New York, 270 Madison Ave.: Taylor & Francis.
37. Ndiaye, C., Fall, M., Ndiaye, M., Sangare, D., & Tall, A. (2014). A review and update of analytical and numerical solutions of the Terzaghi one-dimensional consolidation equation. *Open Journal of Civil Engineering*, 4, 274-284. Retrieved from <http://dx.doi.org/10.4236/ojce.2014.43023>.

- 38.** Ahmed B., (2006). “New laboratory test procedure for the enhanced calibration of constitutive models”. Ph.D. thesis, Georgia Institute of Technology.
- 39.** Mustefa T., (2016). “Comparison of conventional incremental load and constant rate of strain consolidation test results for red clay of addis ababa”. M.Sc. Thesis Presented to School of Graduate Studies, Addis Ababa University, Addis Ababa.

Simulation of Oedometer test using Finite Element Method

Appendix A

One-dimensional Consolidation (Oedometer) test laboratory results of red clay soil from the selected area of Addis Ababa.

Table: 1A Dial guage readings for both loading and unloading cases of Adisu Gebeya red clay.

Time(min)	Dial guage readings for Loading							Dial guage readings for Unloading				
	7 (kPa)	50 (kPa)	100 (kPa)	200 (kPa)	400 (kPa)	800 (kPa)	1600 (kPa)	1600 (kPa)	800 (kPa)	400 (kPa)	200 (kPa)	100 (kPa)
0	0.078	0.055	0.245	0.386	0.935	1.519	2.169	2.885	2.517	2.406	2.204	2.115
0.25	-	0.0838	0.276	0.778	1.338	1.772	2.29	2.642	2.464	2.27	2.176	2.088
0.5	-	0.0953	0.288	0.79	1.342	1.908	2.47	2.634	2.454	2.264	2.172	2.082
1	-	0.119	0.304	0.808	1.366	1.974	2.51	2.632	2.452	2.256	2.17	2.078
2	-	0.134	0.316	0.826	1.392	2.004	2.556	2.631	2.446	2.253	2.167	2.074
4	-	0.141	0.328	0.844	1.416	2.034	2.598	2.629	2.438	2.246	2.164	2.07
8	-	0.153	0.344	0.858	1.433	2.057	2.74	2.626	2.434	2.239	2.157	2.068
15	-	0.161	0.351	0.87	1.448	2.08	2.774	2.624	2.43	2.234	2.152	2.066
30	-	0.169	0.359	0.884	1.462	2.119	2.799	2.622	2.424	2.228	2.146	2.064
60	-	0.176	0.367	0.895	1.475	2.123	2.826	2.621	2.417	2.222	2.139	2.058
120	-	0.180	0.373	0.906	1.486	2.131	2.837	2.62	2.413	2.218	2.134	2.054
240	-	0.192	0.378	0.922	1.495	2.142	2.85	2.58	2.412	2.213	2.121	2.05
480	-	0.212	0.384	0.927	1.504	2.151	2.876	2.519	2.41	2.208	2.12	2.044
1440	0.055	0.245	0.386	0.935	1.519	2.169	2.885	2.517	2.406	2.204	2.115	2.04

Simulation of Oedometer test using Finite Element Method

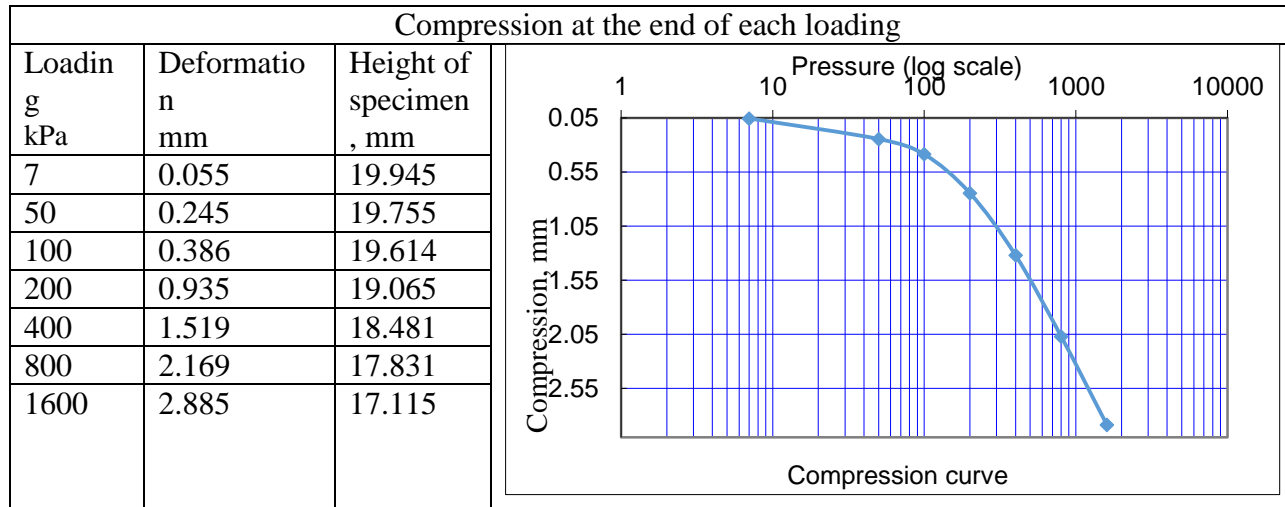


Fig. 1A Compression – Pressure (log scale) curve for Adisu-Gebeya red clay soil.

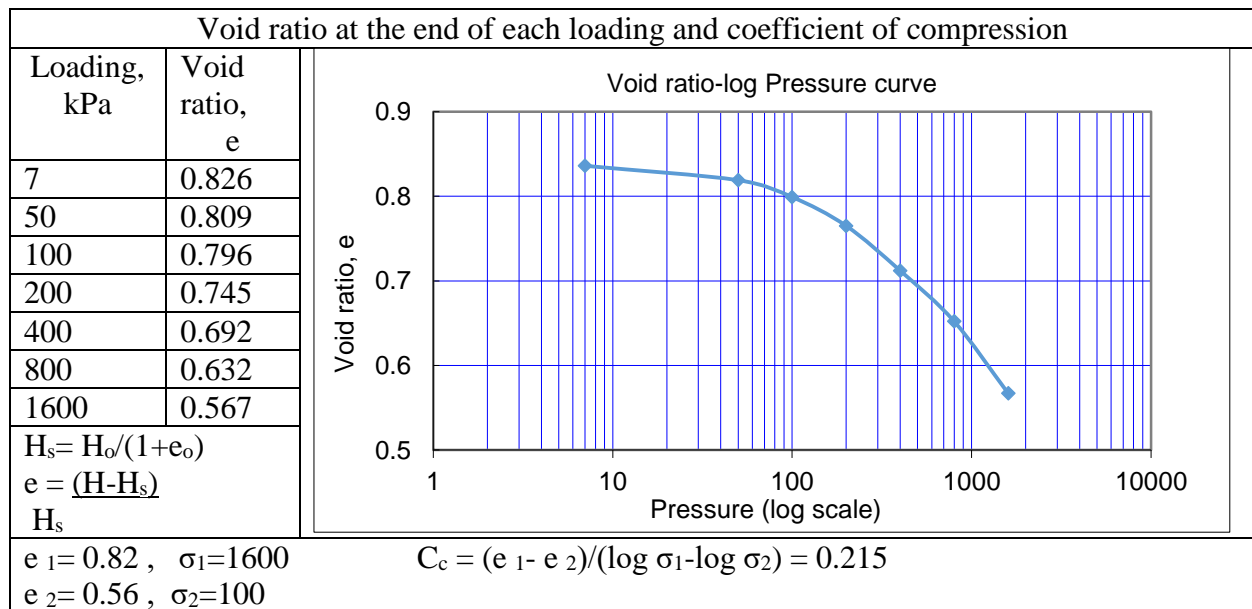


Fig. 2A Void ratio – Pressure (log scale) curve for Adisu-Gebeya red clay soil.

Simulation of Oedometer test using Finite Element Method

Table: 3A Dial gage readings of both loading and unloading cases for kolfe area red clay.

Time(min)	Dial guage readings of Loading							Dial guage readings of Unloading				
	7 (kPa)	50 (kPa)	100 (kPa)	200 (kPa)	400 (kPa)	800 (kPa)	1600 (kPa)	1600 (kPa)	800 (kPa)	400 (kPa)	200 (kPa)	100 (kPa)
0	0.088	0.065	0.268	0.435	1.045	1.642	2.372	3.038	2.515	2.391	2.202	2.11
0.25	-	0.114	0.305	0.768	1.328	1.782	2.31	2.644	2.478	2.3	2.196	2.09
0.5	-	0.143	0.311	0.78	1.332	1.918	2.47	2.628	2.464	2.284	2.172	2.08
1	-	0.166	0.318	0.81	1.356	1.984	2.54	2.626	2.462	2.276	2.17	2.078
2	-	0.177	0.329	0.829	1.382	2.014	2.566	2.623	2.456	2.253	2.167	2.074
4	-	0.186	0.342	0.848	1.406	2.044	2.63	2.619	2.448	2.246	2.164	2.071
8	-	0.193	0.345	0.858	1.423	2.077	2.74	2.616	2.444	2.239	2.157	2.068
15	-	0.209	0.346	0.87	1.438	2.09	2.784	2.614	2.43	2.234	2.152	2.065
30	-	0.216	0.348	0.908	1.452	2.117	2.835	2.612	2.424	2.228	2.146	2.063
60	-	0.226	0.349	0.913	1.465	2.128	2.846	2.611	2.419	2.222	2.139	2.057
120	-	0.243	0.366	0.918	1.486	2.134	2.867	2.6	2.416	2.218	2.137	2.052
240	-	0.255	0.373	0.926	1.495	2.195	2.85	2.57	2.412	2.214	2.123	2.051
480	-	0.261	0.393	0.931	1.514	2.253	2.876	2.53	2.398	2.206	2.12	2.047
1440	0.065	0.268	0.435	1.045	1.642	2.372	3.038	2.515	2.391	2.202	2.11	2.044

Simulation of Oedometer test using Finite Element Method

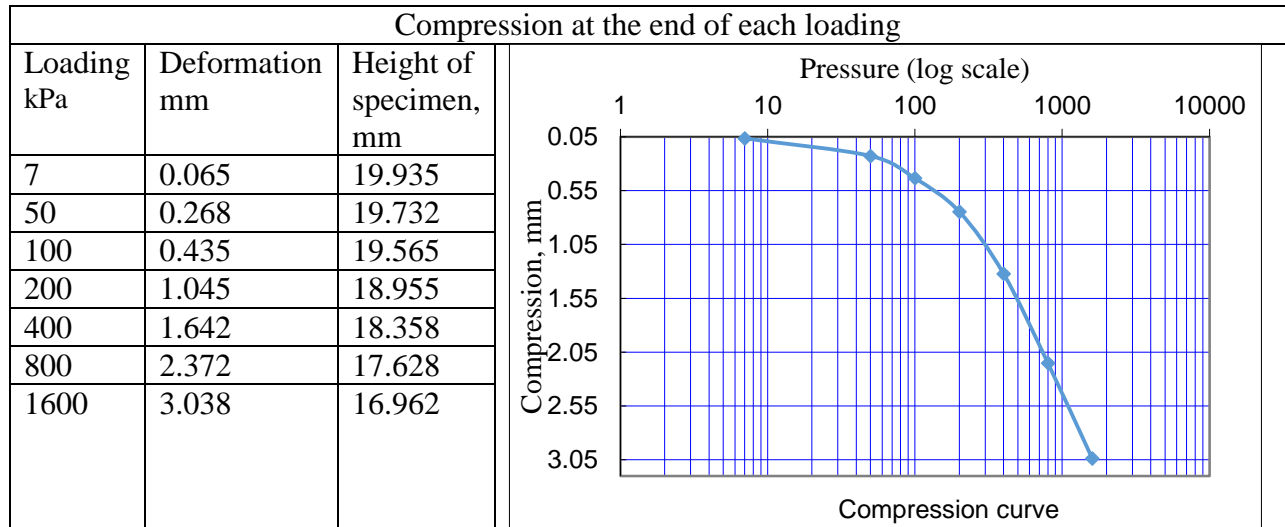


Fig. 3A Void ratio – Pressure (log scale) curve for Kolfe area red clay soil.

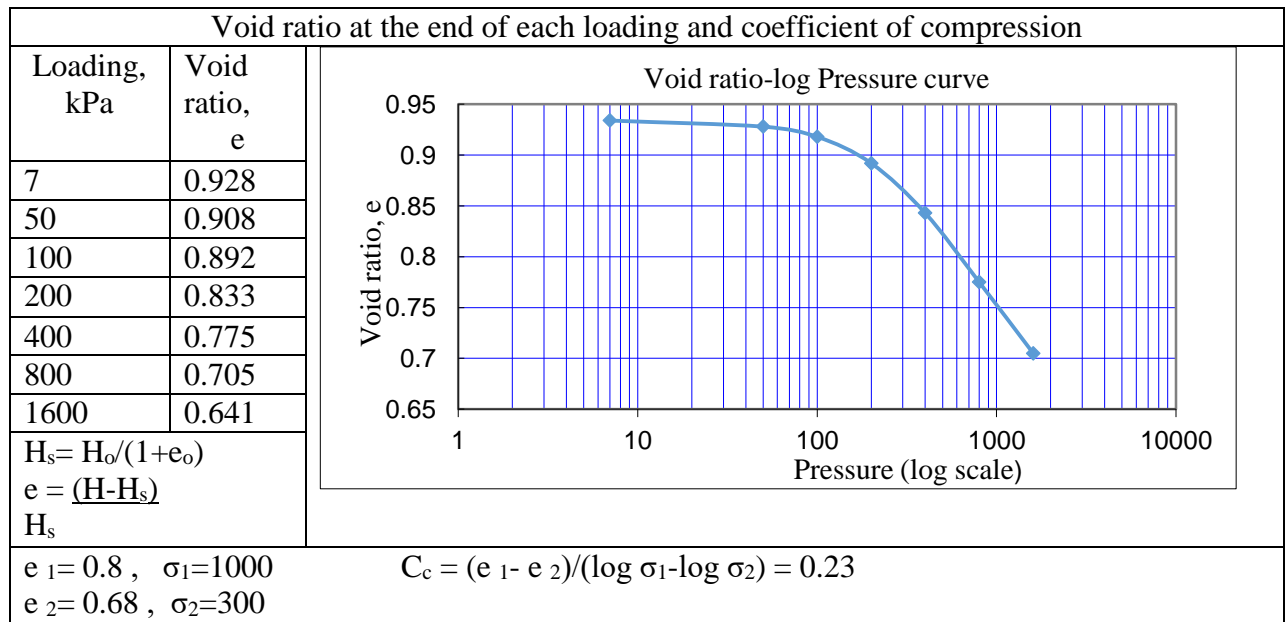


Fig. 4A Void ratio – Pressure (log scale) curve for Kolfe area red clay soil.

Appendix B

Void ratio versus Log pressure curves and preconsolidation pressure (P_c) determination.

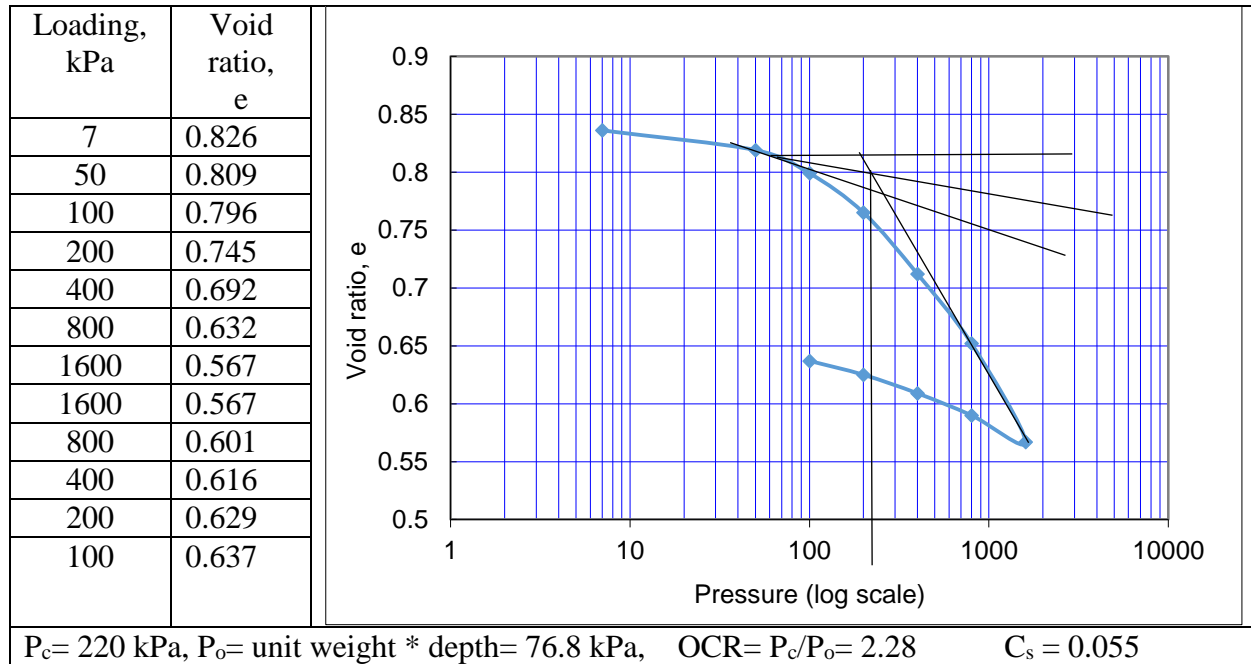


Fig. 1B Determination of pre-consolidation pressure, P_c and over consolidation ratio, OCR using Casagrande method for Adisu Gebeya Red clay.

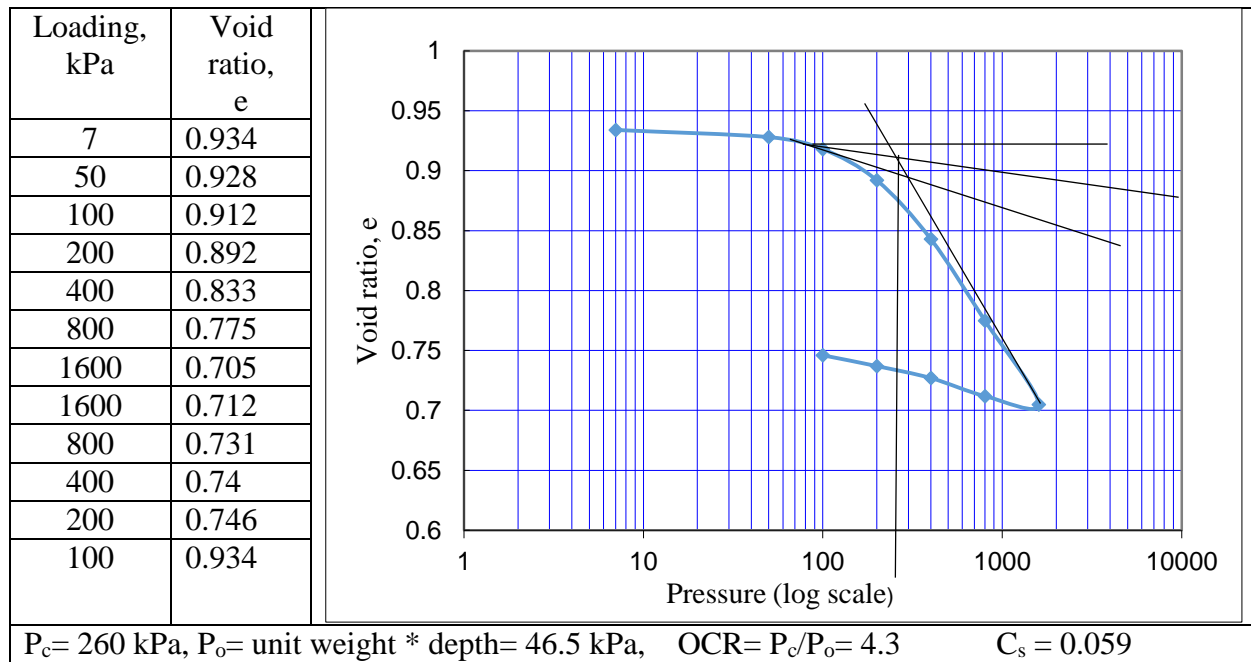


Fig. 2B Determination of pre-consolidation pressure, P_c and over consolidation ratio, OCR using Casagrande method for Kolfe Red clay.

Appendix C

The mean effective stress is related with the plastic volumetric strain with the following equation to generate the cap hardening curve.

$$\epsilon_v^p = \frac{\lambda - \kappa}{1 + e_0} \ln \frac{P'}{P'0} = \frac{Cc - Cs}{2.3(1 + e_0)} \ln \frac{P'}{P'0} \quad \& \quad x = \frac{Cc - Cs}{2.3(1 + e_0)}$$

Table 1C: Cap hardening behaviour for both Adisu Gebeya and Kolfe area red clay soils.

Location	Compression index(Cc)	Re-compression index (Cr)	Expansion index(Cs)	Initial void ratio, (e0)	Case-1, x	Case-2, x	Case-3, x
Adisu Gebeya area	0.215	0.0307	0.055	0.831	0.0068	0.0442	0.0511
Kolfe area	0.23	0.0329	0.059	0.934	0.0073	0.0473	0.0546
Rufael area	0.15	0.0214	0.0204	0.778	0.0052	0.0214	0.0367

Table 2C: Plastic volumetric strain Vs mean effective stress for Adisu Gebeya area for case-1

ϵ_v^p	p
0	220
0.0225	397.63
0.0415	650.62
0.0525	926.71
0.0635	1230.61
0.0775	1845.15
0.0925	2796.2
0.115	4668.7
0.135	7008.38
0.155	10239.57

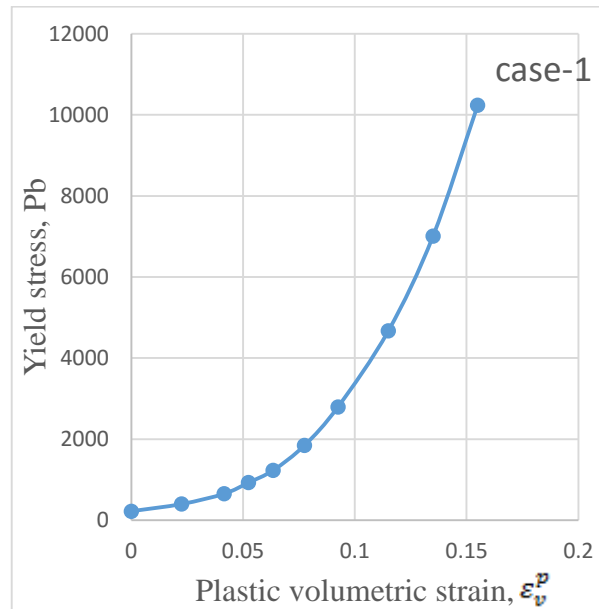


Fig. 1C: Cap hardening curve for Adisu Gebeya red clay sample case-1

Table 3C: Plastic volumetric strain Vs mean effective stress for Adisu Gebeya area for case-2

ϵ_v^p	p
0	220
0.0225	475.21
0.0415	688.36
0.0525	919.91
0.0635	1235.01
0.0775	1896.32
0.0925	3356.37
0.115	6315.87
0.135	10531.96
0.155	16387.05

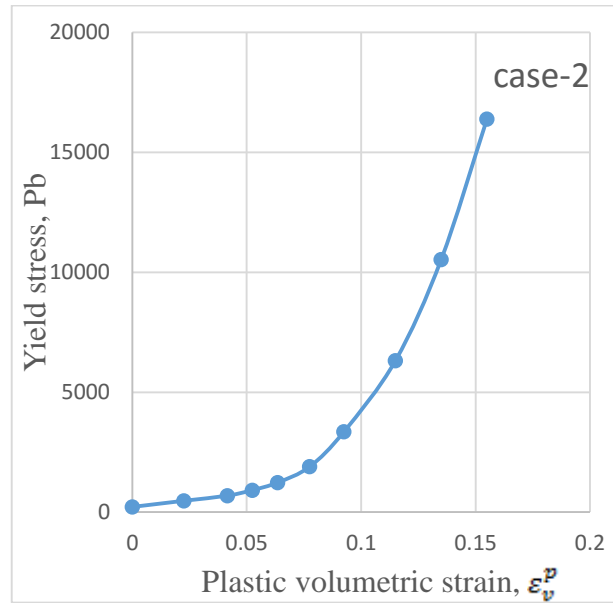


Fig. 2C: Cap hardening curve for Adisu Gebeya red clay sample case-2

Table 4C: Plastic volumetric strain Vs mean effective stress for Adisu Gebeya area for case-3

ϵ_v^p	p
0	220
0.0225	532.65
0.0415	987.6
0.0525	1448.3
0.0635	2279.87
0.0775	4123.41
0.0925	6764.92
0.115	11587.02
0.135	16781.05
0.155	23512.43

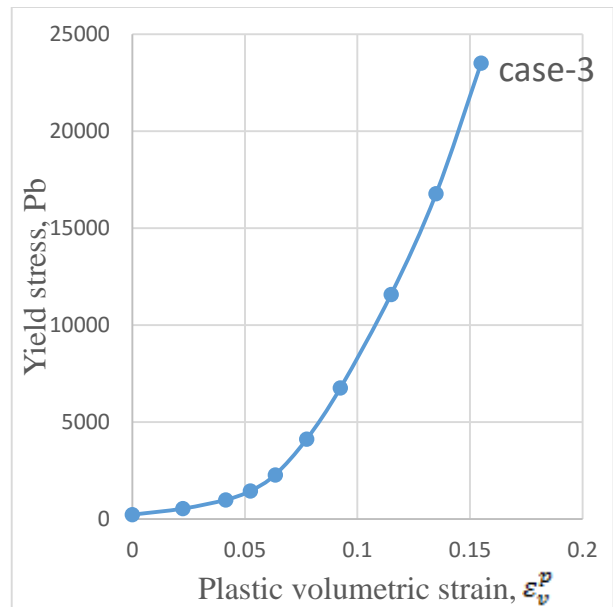


Fig. 3C: Cap hardening curve for Adisu Gebeya red clay sample case-3

Table 5C: Plastic volumetric strain Vs mean effective stress for Kolfe area case-1

ϵ_v^p	p
0	260
0.0225	359.34
0.0415	589.36
0.0525	784.86
0.0635	1045.2
0.0775	1504.99
0.0925	2224.24
0.115	3996.24
0.135	6727.4
0.155	11325.09

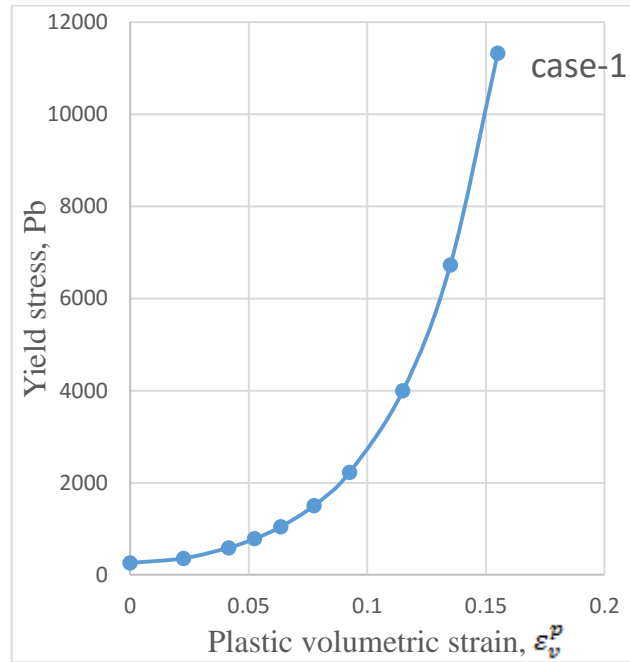


Fig. 4C: Cap hardening curve for kolfe area red clay sample case-1

Table 6C: Plastic volumetric strain Vs mean effective stress for Kolfe area case-2

ϵ_v^p	p
0	260
0.0225	587.62
0.0415	985.31
0.0525	1552.74
0.0635	2178.21
0.0775	4041.37
0.0925	6625.12
0.115	11789.65
0.135	18521.37
0.155	26682.43

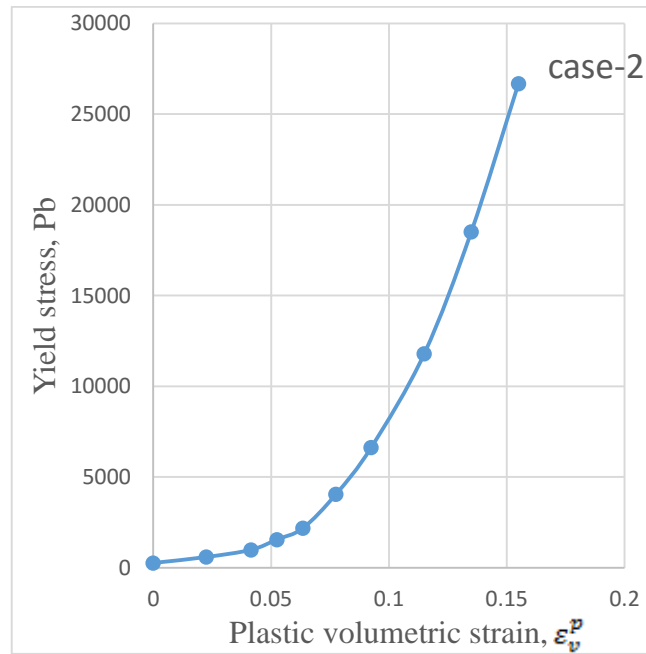


Fig. 5C: Cap hardening curve for kolfe area red clay sample case-2

Table 7C: Plastic volumetric strain Vs mean effective stress for Kolfe area case-3

ϵ_v^p	p
0	260
0.0225	687.62
0.0415	1385.31
0.0525	1852.74
0.0635	2978.21
0.0775	4741.37
0.0925	7625.12
0.115	13789.65
0.135	20521.37
0.155	28682.43

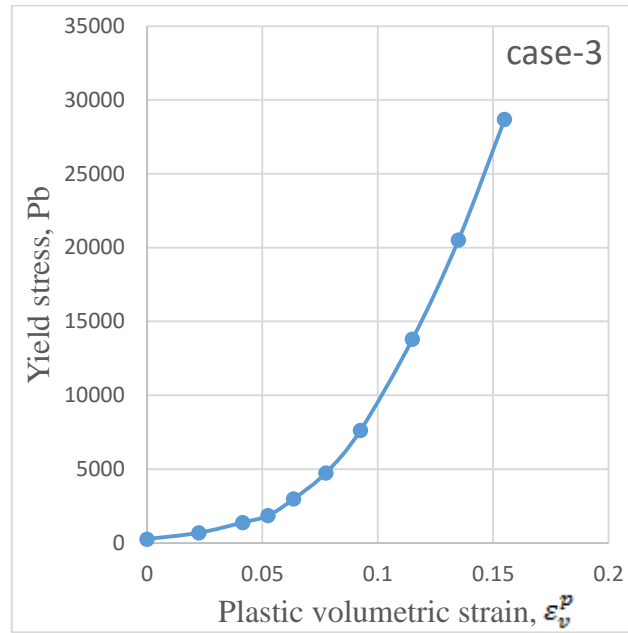


Fig. 6C: Cap hardening curve for kolfe area red clay sample case-3

Table 8C: Plastic volumetric strain Vs mean effective stress for Rufael areared clay case-1

ϵ_v^p	p
0	295
0.0225	412.35
0.0415	670.62
0.0525	956.71
0.0635	1330.61
0.0775	1945.15
0.0925	2896.2
0.115	4768.7
0.135	7108.38
0.155	11239.57

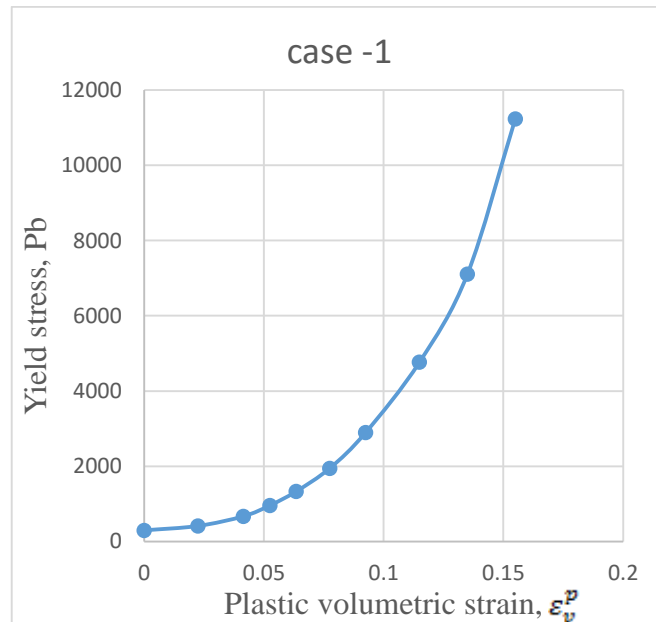


Fig. 7C: Cap hardening curve for Rufael area red clay sample case-1

Table 9C: Plastic volumetric strain Vs mean effective stress for Rufael area case-2

ϵ_v^p	p
0	295
0.0225	495.21
0.0415	698.36
0.0525	979.91
0.0635	1335.01
0.0775	1996.32
0.0925	3456.37
0.115	6415.87
0.135	11531.96
0.155	17387.05

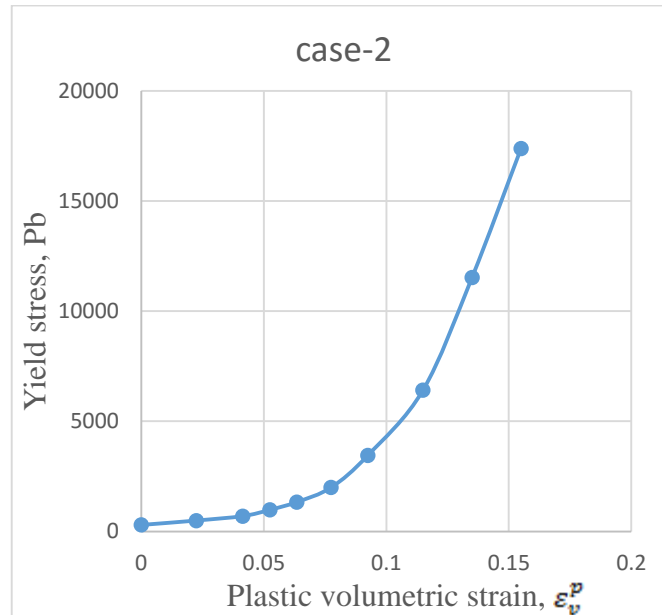


Fig. 8C: Cap hardening curve for Rufael area red clay sample case-2

Table 10C: Plastic volumetric strain Vs mean effective stress for Rufael area case-3

ϵ_v^p	p
0	295
0.0225	542.65
0.0415	1087.6
0.0525	1548.3
0.0635	2379.87
0.0775	4223.41
0.0925	6864.92
0.115	12587.02
0.135	17781.05
0.155	24512.43

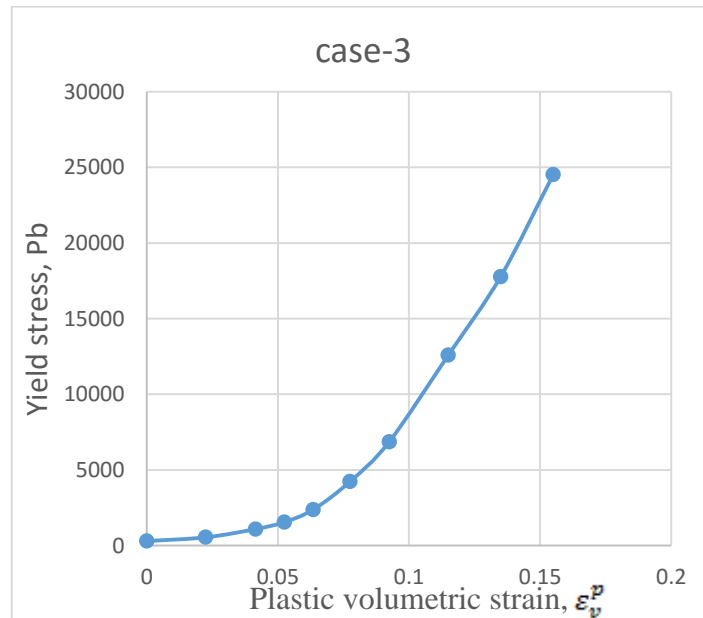


Fig. 9C: Cap hardening curve for Rufael area red clay sample case-3

Appendix D

Finite element method results

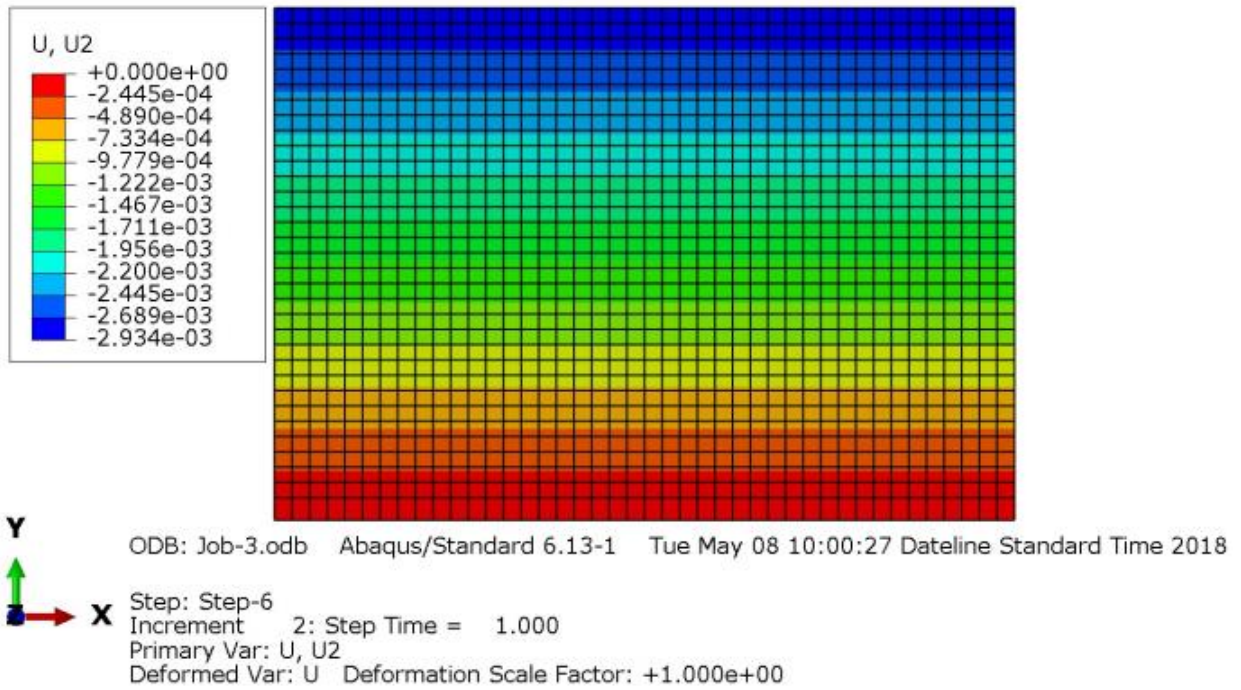


Fig. 1D FEM result for Adisu Gebeyaarea red clay case-1

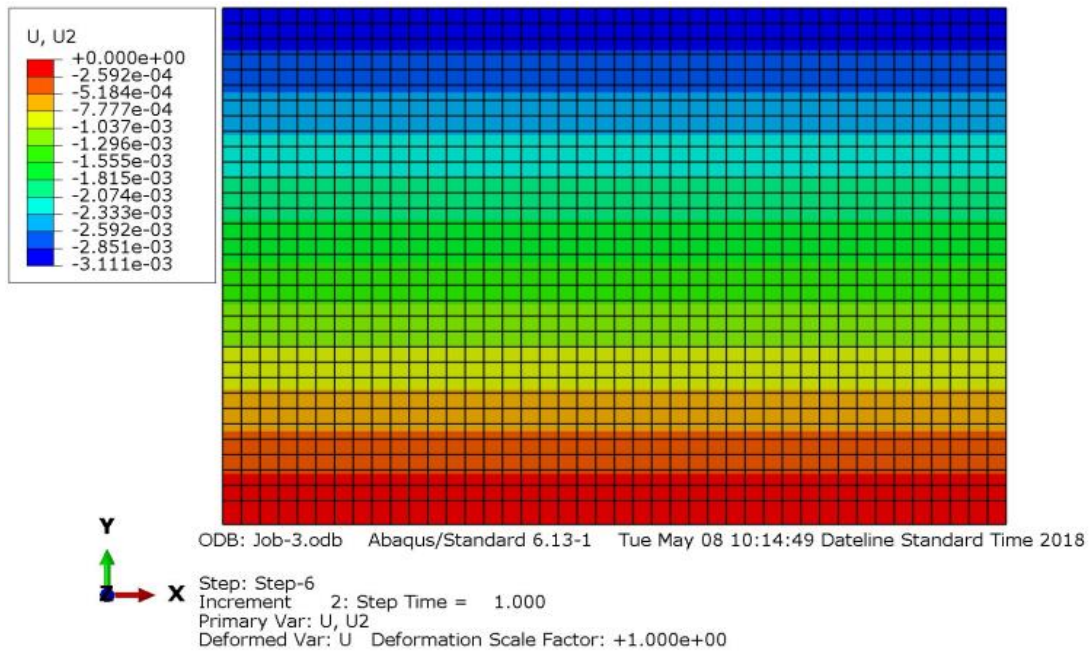


Fig. 2D FEM result for Adisu Gebeyaarea red clay case-2

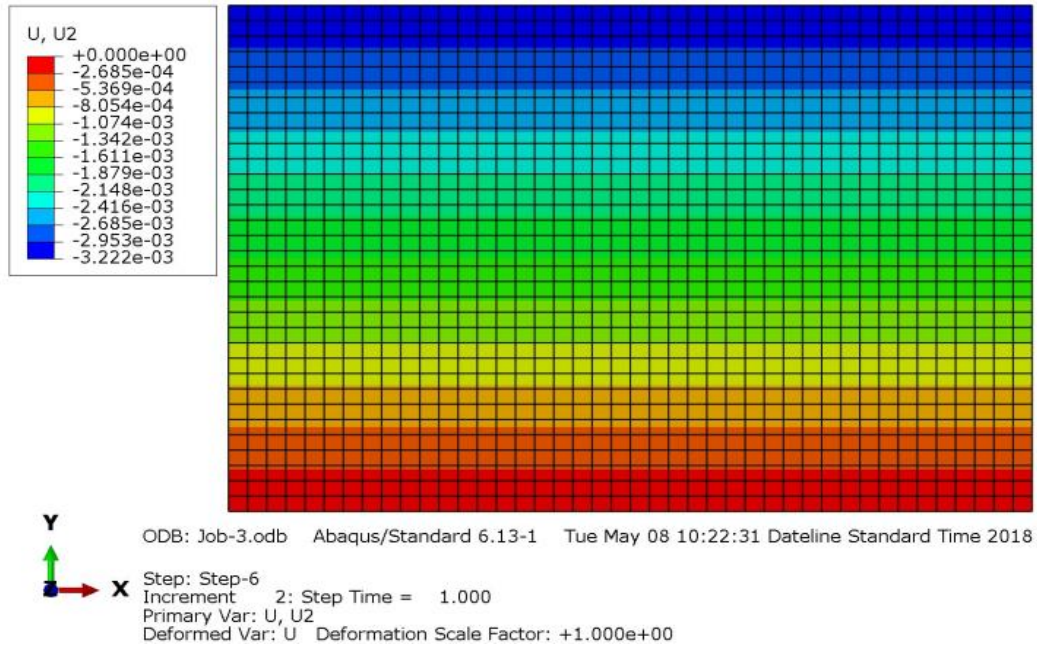


Fig. 3D FEM result for Adisu Gebeyaarea red clay case-3

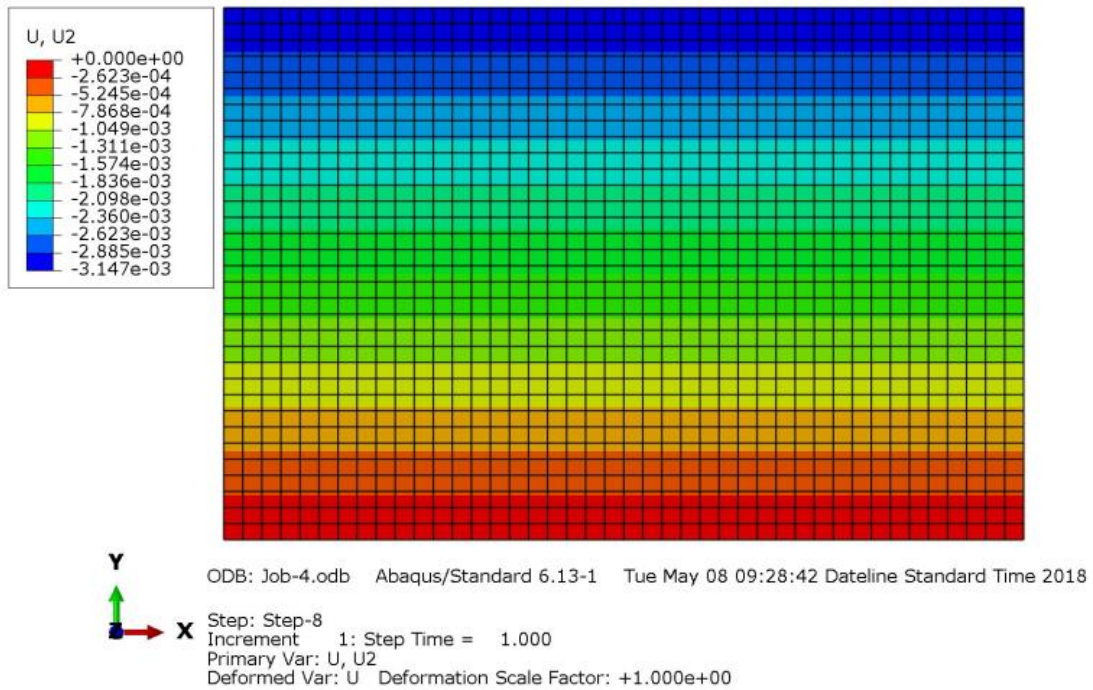


Fig. 4D FEM result for Kolfe area red clay case-1

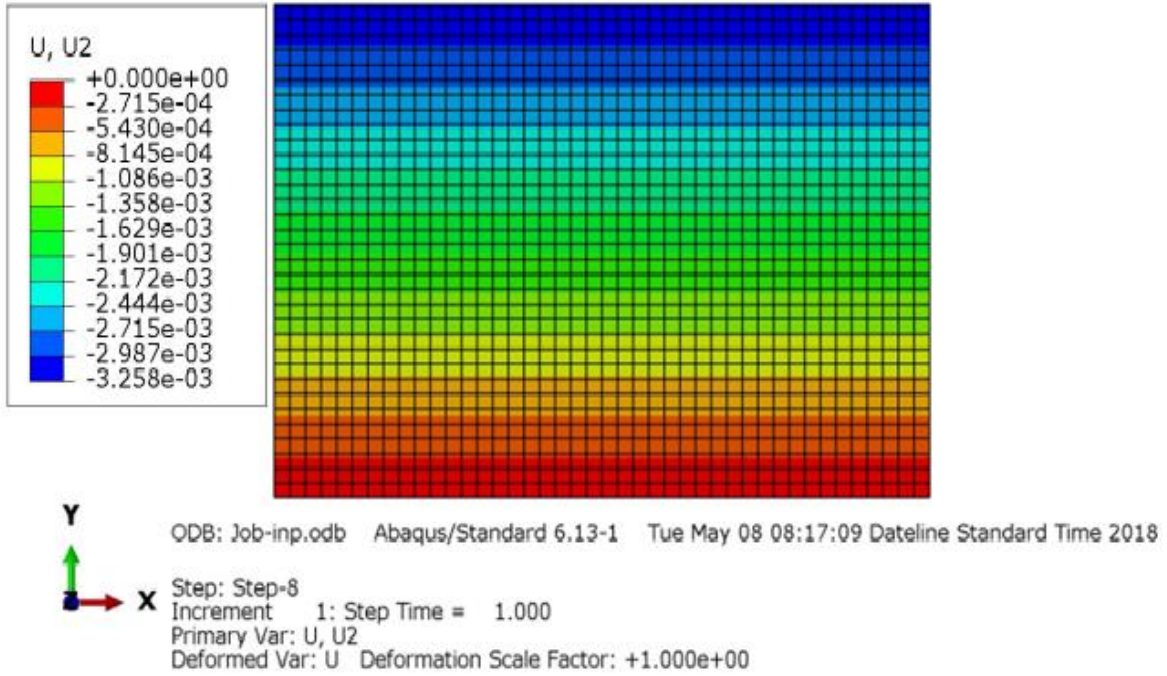


Fig. 5D FEM result for Kolfe area red clay case-2

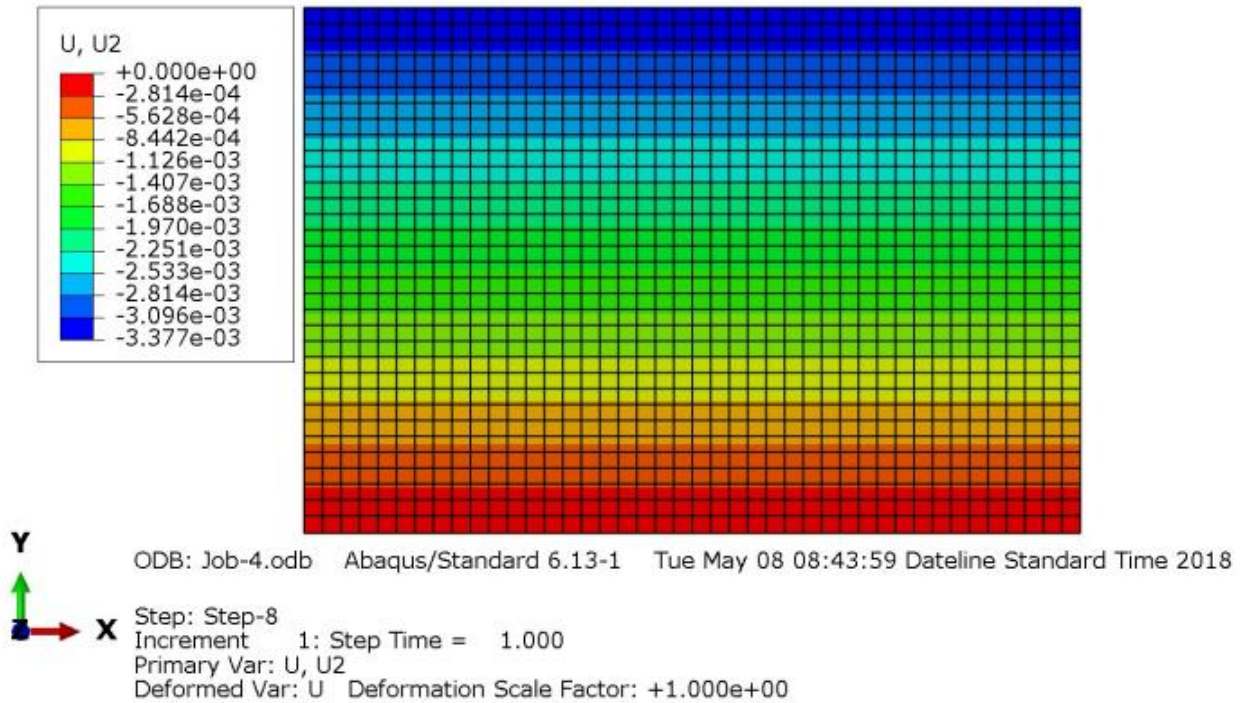


Fig. 6D FEM result Kolfe area red clay case-3

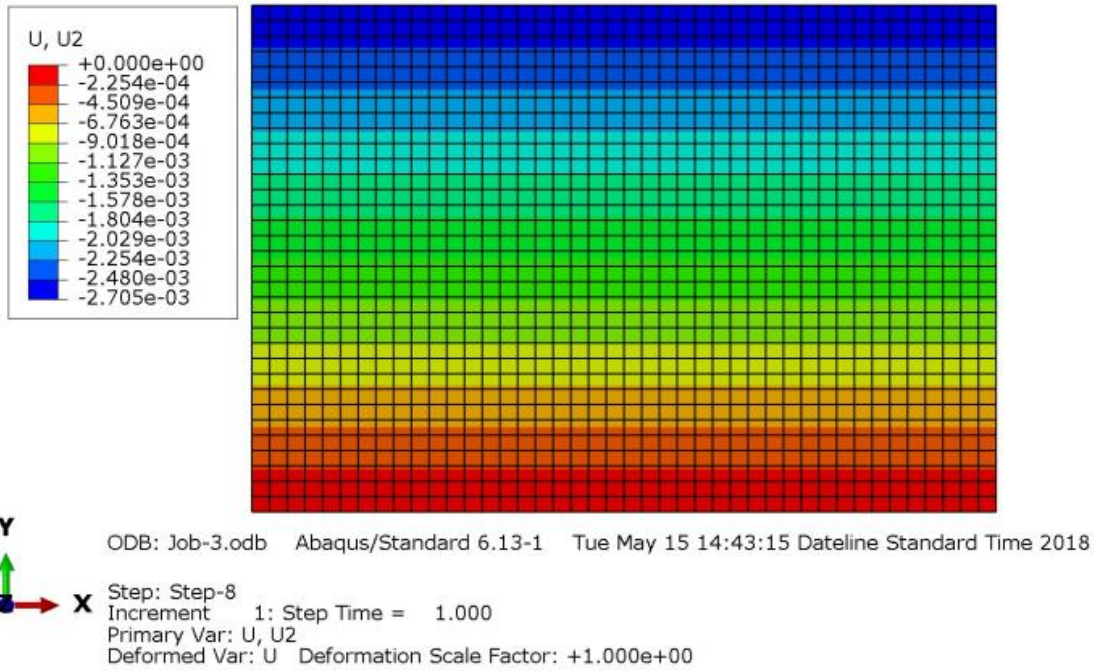


Fig. 7D FEM result Rufaelarea red clay case-1

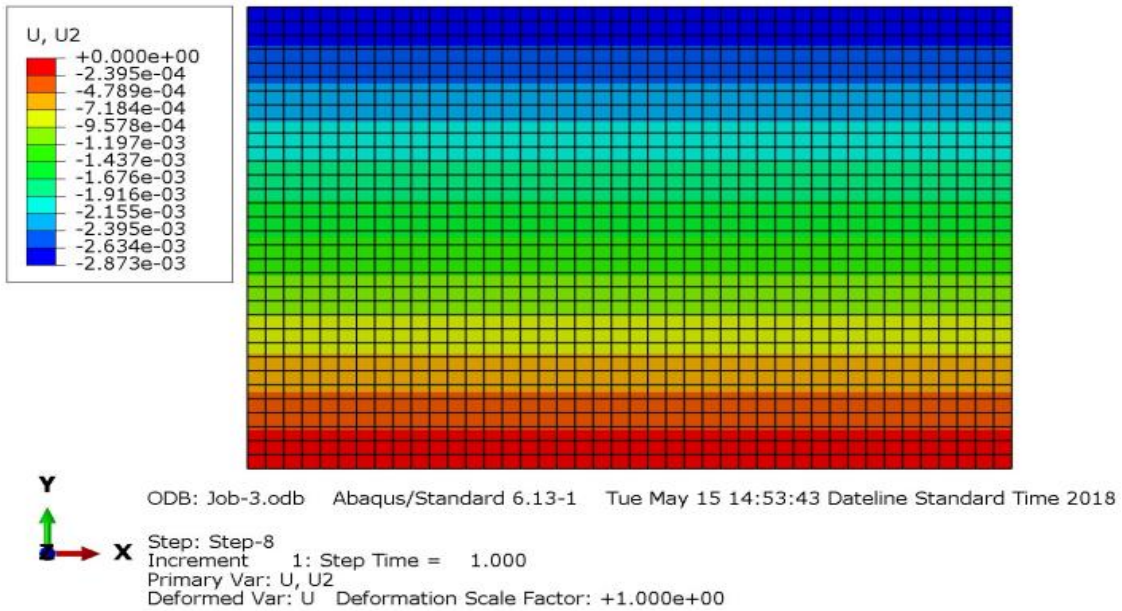


Fig. 8D FEM result Rufaelarea red clay case-2

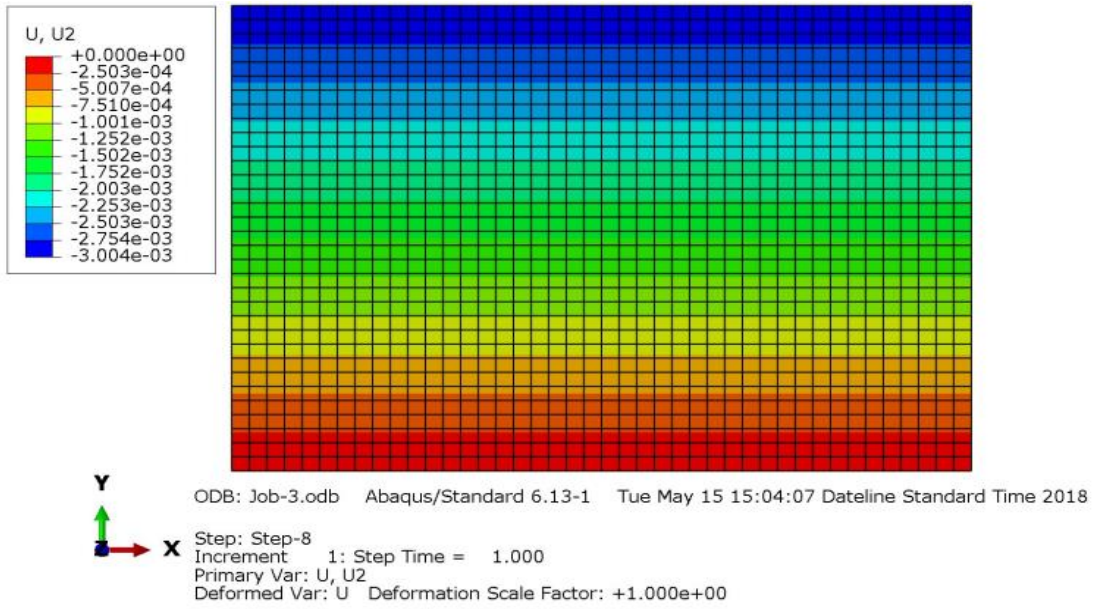


Fig. 9D FEM result Rufaelarea red clay case-3